Electrical Oscillations in Wind Power Plants

Modeling, Control, and Mitigation

Ebrahimzadeh, Esmaeil

DOI (link to publication from Publisher):
10.5278/vbn.phd.eng.00060

Publication date:
2018

Document Version
Publisher's PDF, also known as Version of record

ELECTRICAL OSCILLATIONS IN WIND POWER PLANTS

MODELING, CONTROL, AND MITIGATION

BY
ESMAEIL EBRAHIMZADEH

DISSERTATION SUBMITTED 2018

AALBORG UNIVERSITY
DENMARK

ELECTRICAL OSCILLATIONS IN WIND POWER PLANTS

MODELING, CONTROL, AND MITIGATION

by
Esmaeil Ebrahimzadeh

AALBORG UNIVERSITY
DENMARK

Dissertation submitted 2018

.

Dissertation submitted: 2018

PhD supervisor: Professor Frede Blaabjerg
Aalborg University

Assistant PhD supervisor: Professor Claus Leth Bak
Aalborg University

PhD committee: Zhe Chen (chairman)
Aalborg University

Professor Marta Molinas
Norwegian University of Science and Technology

Professor Jianhui Wang
Argonne National Laboratory

PhD Series: Faculty of Engineering and Science, Aalborg University

Department: Department of Energy Technology

ISSN (online): 2446-1636
ISBN (online): 978-87-7210-173-6

Published by:
Aalborg University Press
Langagervej 2
DK – 9220 Aalborg Ø
Phone: +45 99407140
aauf@forlag.aau.dk
forlag.aau.dk

Printed in Denmark by Rosendahls, 2018

ENGLISH SUMMARY

Nowadays, the amount of integration of Wind Turbines (WTs) and Wind Power Plants (WPPs) into the electrical grid is increasing. Besides the advantages like sustainability, eco-friendly, and controllability, a high penetration of WPPs is challenging the stability, reliability, and power quality of the electrical grid. Among power quality issues, harmonics and electrical oscillations around and above the fundamental frequency are common phenomena in WPPs and gaining more and more attention. In the literature, these electrical oscillations have been called different names such as harmonic stability, small signal stability, dynamic stability, harmonic resonance, dynamic resonance, or electromagnetic transient stability. This project is focusing on modeling, analysis, control, design, and mitigation of such electrical oscillations in WPPs. In this regard, comprehensive research are done about electrical modeling of WTs and power electronic converters, harmonics and resonances, as well as optimization and mitigation of the problem.

As time-domain simulation analysis has a high computational burden for large systems, in this thesis, a WPP is modelled in the linearized frequency-domain by a Multi-Input Multi-Output (MIMO) transfer function matrix. The oscillatory modes and electrical resonances of the WPP are identified by the determinant of the MIMO matrix. The effects of the various phenomena on electrical oscillations, including the number of WTs, grid Short-Circuit Ratio (SCR), cable lengths, and controller bandwidths, are discussed.

In order to find the main source of the oscillations and resonances, Participation Factor (PF) and sensitivity analysis based on the MIMO matrix are presented. PF analysis can locate which WT can contribute more in the electrical oscillations or which bus can excite the resonances. A bus with the largest PF can be selected as the best place for doing active or passive damping activities.

In order to reduce the electrical oscillations and resonance probability, an optimum design procedure in the frequency-domain is presented to put the oscillatory modes of the WPP into the desired locations with acceptable damping. The optimum design can guarantee a stable operation of the WPP and damp the oscillations, while it is also robust against variations in the system.

Non-linear time-domain simulations of a 400-MW WPP in the PSCAD/EMTDC software environment are provided to confirm the effectiveness of the proposed model, analysis, and design.

Keywords: Wind Power Plant (WPP), Wind Turbine (WT), Modeling, Participation Factor (PF) Analysis, Control, Design, Optimization, Electrical Oscillations, Harmonic Stability, Small Signal Stability, Harmonic Resonance, Electromagnetic Transient Stability.

DANSK RESUME

I dag er integrationen af vindmøller (WTs) og vindkraftværker (WPP'er) i elnettet stigende. Ud over fordele som bæredygtighed, miljøvenlighed og kontrollerbarhed udfordrer en høj indtrængning af WPP'er stabiliteten, pålideligheden og strømkvaliteten af det elektriske net.

Foruden grundtonefrekvensen er harmoniske svingninger er kendt fænomen i WPP'er som medfører reduceret strømkvaliteten, hvilket har givet en stadig større opmærksomhed blandt forskere på dette område. I litteraturen er disse elektriske oscillationer blevet kaldt forskellige navne, blandt andet harmonisk stabilitet, lavsignals stabilitet, dynamisk stabilitet, harmonisk resonans, dynamisk resonans eller elektromagnetisk stabilitet. Dette projekt fokuserer på modellering, analyse, styring, design og begrænsning af sådanne elektriske svingninger i WPP'er. I det henseende, er der udført et omfattende studie vedrørende elektrisk modellering af WT'er og effektelektroniske omformere, harmoniske svingninger og resonanser samt optimering og udbedring af førnævnte problemer.

Da simuleringer i tidsdomænet har en høj beregningsbyrde for store systemer, vil WPP'er blive modelleret i det lineære frekvensdomæne ved hjælp af Multi-input Multi-output (MIMO) overføringsfunktionsmatricer. De oscillerende tilstande samt elektriske resonanser forbundet med WPP'en identificeres ved brug af MIMO-matricens determinant. Effekten af de forskellige fænomener på de elektriske oscillationer, herunder antallet af WT'er, kortslutningsforholdet (SCR), kabellængder og regulatorbåndbredde analyseres og diskuteres.

For at identificere hovedkilden til oscillationerne og resonanserne præsenteres deltagelses-faktoren (PF) der udformeren følsomhedsanalyse baseret på MIMO-matrixen. Analyse af PF kan lokalisere, hvilken WT der bidrager mest til de elektriske svingninger, samt hvilke elektriske busser der er ansvarshavende for at excitere resonanser. En bus med den største PF kan vælges som det bedste sted for aktiv eller passiv dæmpning.

For at reducere elektriske oscillationer og sandsynligheden for resonans, præsenteres en optimal design-procedure for at sikre at WPP's svingningsmæssige tilstande er placeret i et ønsket frekvensområde med en acceptabel dæmpning. Det optimale design kan garantere en stabil drift af WPP'en og dæmpe oscillationerne, samtidig med at det er robust mod forstyrrelser i el-systemet.

Ikke-lineære tidsdomæne-simuleringer af en WPP med en udgangseffekt på 400 MW er udført i PSCAD / EMTDC-softwaremiljøet og inkluderet for at bekræfte effektiviteten af den foreslåede model, systemets analyse og design.

PUBLICATIONS IN THESIS

Peer-reviewed: Four IEEE Journals + Two IEEE Conferences

1) **E. Ebrahimzadeh**, F. Blaabjerg, X. Wang, and C. L. Bak, "Harmonic stability and resonance analysis in large PMSG-based wind power plants," *IEEE Transactions on Sustainable Energy*, vol. 9, no. 1, pp. 12-23, Jan. 2018.

2) **E. Ebrahimzadeh**, F. Blaabjerg, X. Wang, C. L. Bak, T. Lund, G. K. Andersen, C. G. Suárez, and J. Berg "Small signal modeling of wind farms," *in Proc. of IEEE ECCE Conference*, USA, 2017, pp. 1-7.

3) **E. Ebrahimzadeh**, F. Blaabjerg, X. Wang, and C. L. Bak "Bus participation factor analysis for harmonic instability in power electronics based power systems," Early access *in IEEE Transaction on Power Electronics*.

4) **E. Ebrahimzadeh**, F. Blaabjerg, X. Wang, and C. L. Bak, "Dynamic resonance sensitivity analysis in wind farms," *in Proc. of IEEE PEDG Conference*, Brazil, 2017, pp. 1-6.

5) **E. Ebrahimzadeh**, F. Blaabjerg, X. Wang, and C. L. Bak "Optimum design of power converter current controllers in power electronics based power systems," *Submitted* to *IEEE Transactions on Industry Applications*.

6) **E. Ebrahimzadeh**, F. Blaabjerg, X. Wang, and C. L. Bak, "Reducing harmonic instability and resonance problems in PMSG based wind farms," *IEEE Journal of Emerging and Selected Topics in Power Electronics*, vol. 6, no. 1, pp. 73-83, Mar. 2018.

PUBLICATIONS DURING PHD

Peer-reviewed: +12 Journal Articles, +9 Conference Papers, +1 Book Chapter

Peer-reviewed Journals:

1) **E. Ebrahimzadeh**, F. Blaabjerg, X. Wang, and C. L. Bak, "Harmonic stability and resonance analysis in large PMSG-based wind power plants," *IEEE Transactions on Sustainable Energy*, vol. 9, no. 1, pp. 12-23, Jan. 2018.
2) **E. Ebrahimzadeh**, F. Blaabjerg, X. Wang, and C. L. Bak, "Reducing harmonic instability and resonance problems in PMSG based wind farms," *IEEE Journal of Emerging and Selected Topics in Power Electronics*, vol. 6, no. 1, pp. 73-83, Mar. 2018.

3) **E. Ebrahimzadeh**, F. Blaabjerg, X. Wang, and C. L. Bak "Optimum design of power converter current controllers in power electronics based power systems," *Submitted* to *IEEE Transactions on Industry Applications*.
4) **E. Ebrahimzadeh**, F. Blaabjerg, C. L. Bak, and X. Wang "Bus participation factor analysis for harmonic instability in power electronics based power systems," Early access *in IEEE Transaction on Power Electronics*.
5) **E. Ebrahimzadeh**, S. Farhangi, H. Iman-Eini, and F. Blaabjerg "Modulation technique for four-leg voltage source Inverter without a look-up table," *IET Power Electronics*, vol. 9, no. 4, pp. 648-656, Mar. 2016.
6) S. Golestan, **E. Ebrahimzadeh**, J. Guerrero, J. C. Vasquez, and F. Blaabjerg, "An adaptive least-error squares filter-based phase-locked loop for synchronization and signal decomposition purposes," *IEEE Transaction on Industrial Electronics*., vol. 64, no. 1, pp. 336-346, Jan. 2017.
7) J. Mohammadi, S. Afsharnia, **E. Ebrahimzadeh**, and F. Blaabjerg, "An enhanced LVRT scheme for DFIG-based WECSs under both balanced and unbalanced grid voltage sags," *Electric Power Components and Systems Journal*, vol. 45, no. 11, pp. 1242-1252, Jul. 2017.
8) E. Z. Bighash, S. M. Sadeghzadeh, **E. Ebrahimzadeh**, and F. Blaabjerg, "Improving performance of LVRT capability in single-phase grid-tied PV inverters by a model-predictive controller," *International Journal of Electrical Power & Energy Systems*, vol. 98, no. 2, pp. 176-188, Jun. 2018.
9) E. Z. Bighash, S. M. Sadeghzadeh, **E. Ebrahimzadeh**, and F. Blaabjerg, "Adaptive harmonic compensation in residential distribution grid by roof-top PV systems," Early access in *IEEE Journal of Emerging and Selected Topics in Power Electronics*.
10) E. Z. Bighash, S. M. Sadeghzadeh, **E. Ebrahimzadeh**, and F. Blaabjerg, "High quality model predictive control for single phase grid-connected photovoltaic," Early access in *Electric Power Systems Research*.
11) Y. Song, **E. Ebrahimzadeh**, and F. Blaabjerg, "Analysis of high frequency resonance in DFIG-based offshore wind farm via long transmission cable," Early access in *IEEE Transaction on Energy Conversion*.
12) J. Mohammadi, S. Afsharnia, **E. Ebrahimzadeh**, and F. Blaabjerg, "A combined control method for grid side converter of doubly fed induction generator based wind energy conversion systems," submitted to *IET Renewable Power Generation.*

Book Chapter:

1) **E. Ebrahimzadeh** and F. Blaabjerg, "Reactive power role and its controllability in AC power transmission systems ", in *Reactive Power Control in AC Power Systems*, Springer International Publishing, 2017, pp. 117-136.

Peer-reviewed Conferences:

1) **E. Ebrahimzadeh**, F. Blaabjerg, X. Wang, C. L. Bak, T. Lund, G. K. Andersen, C. G. Suárez, and J. Berg "Small signal modeling of wind farms," *in Proc. of IEEE ECCE Conference*, USA, 2017, pp. 1-7.
2) **E. Ebrahimzadeh**, F. Blaabjerg, X. Wang, and C. L. Bak, "Efficient approach for harmonic resonance identification of large wind power plants," *in Proc. IEEE PEDG Conference*, Canada, 2016, pp. 1-7. (Best Paper Award)
3) **E. Ebrahimzadeh**, F. Blaabjerg, X. Wang, and C. L. Bak, "Harmonic instability source identification in large wind farms," *in Proc. of IEEE PES GM Conference*, USA, 2017, pp. 1-5. (Best Paper Award)
4) **E. Ebrahimzadeh**, F. Blaabjerg, X. Wang, and C. L. Bak, "Multi-objective optimization of large wind farm parameters for harmonic instability and resonance conditions," *in Proc. of IEEE COMPEL Conference*, Norway, 2016, pp. 1-8.
5) **E. Ebrahimzadeh**, F. Blaabjerg, X. Wang, and C. L. Bak, "Dynamic resonance sensitivity analysis in wind Farms," *in Proc. of IEEE PEDG Conference*, Brazil, 2017, pp. 1-6.
6) **E. Ebrahimzadeh**, F. Blaabjerg, X. Wang, and C. L. Bak, "Modeling and identification of harmonic instability problems in wind farms," *in Proc. of IEEE ECCE Conference*, USA, 2016, pp. 1-7.
7) P. Hou, **E. Ebrahimzadeh**, X. Wang, F. Blaabjerg, J. Fang, and Y. Wang, "Harmonic stability analysis of offshore wind farm with CCM," *in Proc. of IEEE IECON Conference, China, 2017*, pp. 1-6.
8) E. Z. Bighash, S. M. Sadeghzadeh, **E. Ebrahimzadeh**, and F. Blaabjerg, "LVRT capability of single-phase grid-connected HERIC inverter in PV systems by a look-up table based predictive control," *in Proc. of IEEE IECON Conference, China, 2017*, pp. 1-6.
9) E. Z. Bighash, S. M. Sadeghzadeh, **E. Ebrahimzadeh**, and F. Blaabjerg, "A novel predictive control for single phase grid-connected photovoltaic inverters," *in Proc. of IEEE ECCE Conference*, USA, 2017, pp. 1-7.

ACKNOWLEDGEMENTS

This thesis is fully funded by HARMONY Project (http://www.harmony.et.aau.dk), Department of Energy Technology, Aalborg University. HARMONY stands for "harmonic identification, mitigation and control in power electronics based power systems", which is leaded by Professor Frede Blaabjerg, who has been awarded an ERC Advanced Grant. I am so thankful for him for giving me this opportunity to join an international team of highly-efficient researchers. I would like to give my special thanks again to Prof. Frede Blaabjerg and Prof. Claus Leth Bak for their constructive and efficient comments, continuous supports and suggestions, and technical discussions during this PhD project.

I would like to give my appreciation to Dr. Xiongfei Wang from the Department of Energy Technology, Aalborg University, for his useful discussions and assistance.

I would also like to give many thanks to Philip C. Kjær, Torsten Lund, Gert K. Andersen, and Jens-Jacob Berg, from Vestas Wind Systems A/S, Aarhus, to give me a visiting opportunity to work with them.

Last but not least, my deepest gratefulness is given to my parents for their all support and encouragement.

Esmaeil Ebrahimzadeh
2018
Aalborg University
Aalborg Øst, Denmark

TABLE OF CONTENTS

TABLE OF FIGURES

CHAPTER 1. INTRODUCTION

1.1. BACKGROUND AND MOTIVATION

Nowadays, the proportion of the power electronics converters in the power grid is growing [1] because of the significant use in different industrial and commercial applications like renewable energy sources [2], HVDC [3], FACTS [4], microgrids [5], railway systems [6], and variable-speed drives [7]. The Global Wind Energy Council (GWEC) has been reported that the installed wind capacity has been increased from 23.9 GW in 2001 to 540 GW in 2017, as shown in Figure 1. 1 [8]. According to the GWEC, more than 341,000 wind turbines were generating electrical energy at the end of 2017.

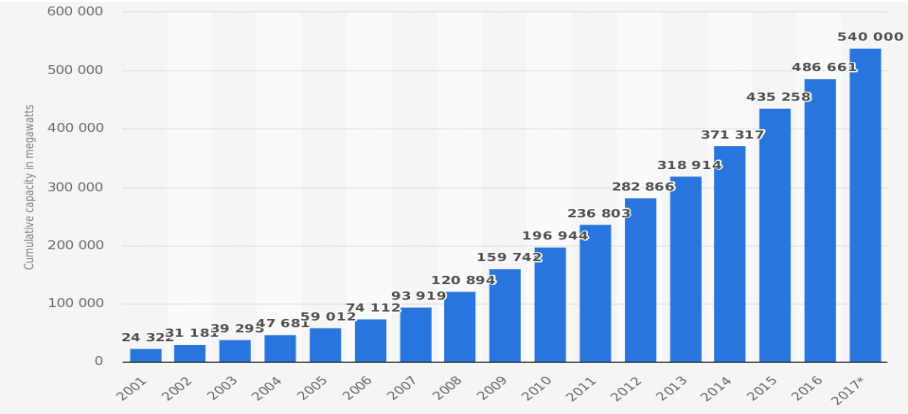

Figure 1. 1: Global cumulative installed wind capacity from 2001 to 2017 [8].

In addition of advantages such as sustainability and economic benefits, high integration of power electronic systems, particularly Wind Power Plants (WPPs), into the power grid is bringing Power Quality (PQ) and reliability problems [9]-[14]. In an ideal case, all voltages and currents in a WPP should be as sinusoidal waveform with a constant fundamental frequency and a nominal magnitude. PQ issues are related to fluctuations in this ideal sinusoidal waveform, which can be in the form of harmonics and oscillations, transients, voltage sags or swells, unbalances, frequency deviation, flicker, and interruption [15]-[20]. Among PQ problems, oscillations are common phenomena in WPPs, which can be in a wide range from lower than 1 Hz until more than a few kilo hertz [21]-[27]. Some recent reports from industries show how unexpected electrical oscillations may happen in the power systems with a high integration of power converters. For example, in a large-scale PV plant in the Dutch distribution network, harmonics and resonance phenomena have tripped the PV

inverters [28]. In a WPP in China (Shanxi province), by increasing the electrical oscillations around 900 Hz, some equipment of the grid-connected power converters was broken [29]. In Denmark and Germany, unexpected shutdowns in offshore WPPs have happened because of the grid distortion amplification and power cable faults [30]- [32]. ABB Corporate Research has also reported the harmonic resonance problems in HVDC connected WPPs [33]. On the other hand, the limited levels of harmonic emission in the power system are limited in the IEC 61000-3-6 standard [34], [35]. Table 1. 1 shows the harmonic emission limits in high voltage buses for higher than 35 kV. As it is shown in Table 1. 1, the limiting levels of oscillations, particularly the high-order oscillations, is very low and strict. All these reported issues highlight the importance of high-frequency oscillation analysis in WPPs, which is going to be conducted in this project.

Table 1. 1: IEC 61000-3-6 standard about harmonic emission limits in high voltage buses higher than 35 kV [35]

Odd harmonics				Even harmonics	
Not multiple of 3		Multiple of 3			
Order h	Harmonic voltage (%)	Order h	Harmonic voltage (%)	Order h	Harmonic voltage (%)
5	2	3	2	2	1.6
7	2	9	1	4	1
11	1.5	15	0.3	6	0.5
13	1.5	21	0.2	8	0.4
17	1	>21	0.2	10	0.4
19	1			12	0.2
23	0.7			>12	0.2
25	0.7				
>25	0.2+ 0.5 ×25/h				

*** THD limit is 6.5 percent.**

1.2. VARIABLE SPEED WIND TURBINE GENERATORS

Wind Turbine (WT) generators can be categorized into fixed-speed and variable-speed wind turbines [36]. In the fixed-speed WTs, any wind fluctuations lead to the electrical power fluctuations and voltage oscillations [37]. Therefore, in recent years, variable-speed WTs, which can operate in the peak efficiency for different wind speeds, are gaining more attention [38]. Doubly Fed Induction Generator (DFIG) with partial-scale converters and Permanent Magnet Synchronous Generator (PMSG) with full-scale converters are two popular types of the variable-speed WTs [36].

1.2.1. DOUBLY FED INDUCTION GENERATOR (DFIG) BASED WIND TURBINE (WT) WITH PARTIAL-SCALE CONVERTERS

The structure of a Doubly Fed Induction Generator (DFIG) with partial-scale converters is shown in Figure 1. 2. The speed of a DFIG based WT may vary in a range of ±30% around the synchronous speed by using an appropriate control for the power converters [39]. The size of the power electronic converters are rated to around

30% of the nominal power of the WT [40]. The Machine Side Converter (MSC) injects an appropriate voltage into the rotor circuit to achieve the Maximum Power Point Tracking (MPPT) [38]. In order to keep the dc-link voltage constant, the Grid Side Converter injects a controlled voltage to the grid [41].

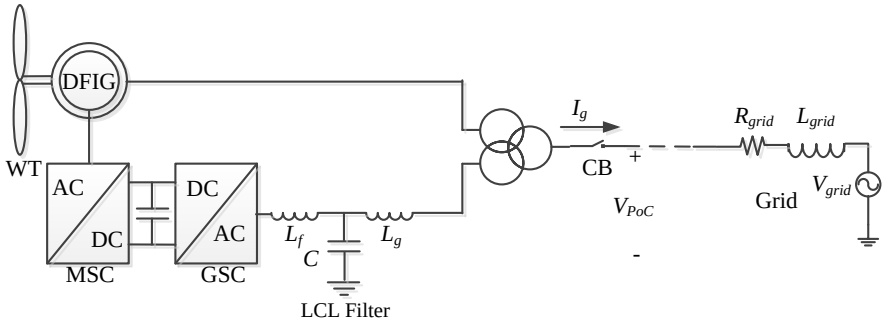

Figure 1. 2: Doubly Fed Induction Generator (DFIG) with partial-scale converters.

1.2.2. PERMANENT MAGNET SYNCHRONOUS GENERATOR (PMSG) BASED WIND TURBINE (WT) WITH FULL-SCALE CONVERTERS

Another popular type of the variable-speed wind turbines is Permanent Magnet Synchronous Generator (PMSG) with full-scale converters, which is shown in Figure 1. 3. In this structure, the size of the back-to-back power converters are rated to the nominal power of the WT, where the GSC is responsible to keep the dc-link voltage constant [42], [43]. By neglecting the small oscillations of the dc-link voltage, the dynamics of the whole WT system is directly related to the dynamics of the GSC [34]. Therefore, the dynamics related to the wind model, turbine, generator, and MSC can be ignored [23].

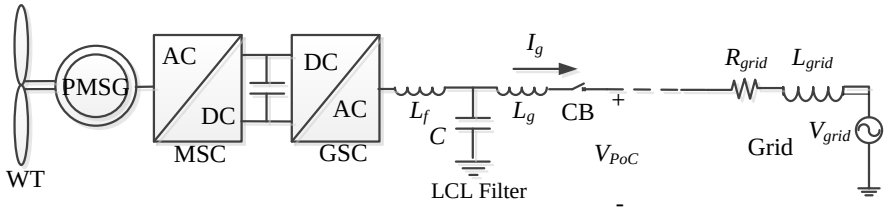

Figure 1. 3: Permanent Magnet Synchronous Generator (PMSG) with full-scale converters.

1.2.3. GRID SIDE CONVERTER (GSC) CONTROL OF WIND TURBINE (WT)

Grid Side Converter (GSC) of a WT can typically be two-level high-power Voltage

Source Converters (VSCs), where the Insulated Gate Bipolar Transistors (IGBTs) are used [44]. The general control of the GSC is shown in Figure 1. 4, including four main parts: dc-link voltage and power controller, Grid synchronization, Current controller, and SPWM [45]. In order to control the dc-link voltage and the injected reactive power, the current references ($I_{ref\text{-}d}$ and $I_{ref\text{-}q}$) are generated and the output currents (I_d and I_q) of the converters are controlled by the PI controllers:

$$G_{cont} = K_p + \frac{K_i}{s} \tag{1.1}$$

The Grid synchronization loops like Phase-Locked Loops (PLLs) estimate the phase angle of the PoC voltage (θ) [46]. The estimated angle is used in the Park transformation to make all the conversions between the *dq* and *abc* reference frames. The final switching signals of the IGBTs are generated by the Sinusoidal Pulse Width Modulation (SPWM). In Figure 1. 4, the time-delay of the discrete control and the SPWM can be modeled by the pade approximation [47] as

$$G_{delay} = e^{-T_d s} \approx \frac{1 - 0.5T_d s}{1 + 0.5T_d s} \tag{1.2}$$

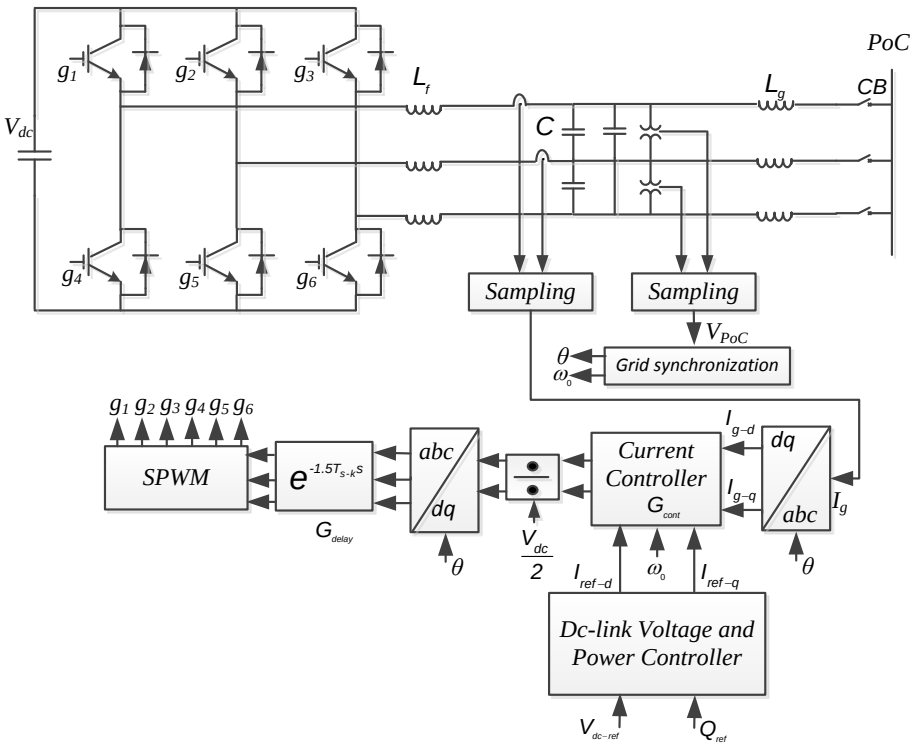

Figure 1. 4: Voltage Source Inverters (VSC), which are typically used in the Wind Turbine (WT) systems.

1.3. ELECTRICAL OSCILLATIONS

Electrical oscillations in the WPP can be increased due to instability in the system or disturbance amplification by resonances of the system [26], [30], [34]. As it can be seen from Figure 1. 5, very low-frequency oscillations are related more to the generator and mechanical devices [48] and the oscillations around the grid frequency and higher than are related to the power converters and their controllers [39], [49].

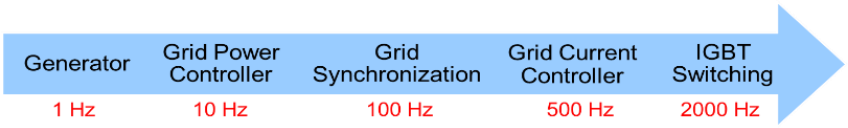

(a) The wide frequency range of oscillations in a Wind Power Plant (WPP).

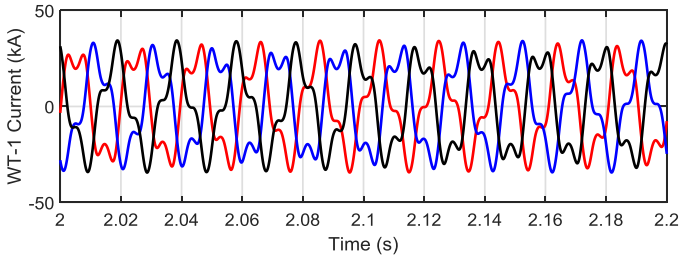

(b) Electrical oscillations around the fundamental frequency, resulting from the interactions between grid synchronization control loops [84].

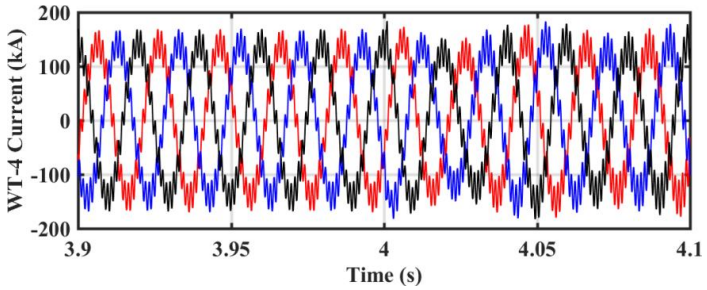

(c) Electrical oscillations above the fundamental frequency, resulting from the interactions between current controllers.

Figure 1. 5: Electrical oscillations in Wind Power Plants (WPPs).

electromechanical oscillations in low-frequency range has been studied well in the conventional power systems [50], [51]. However, it has not been paid much attention to analyze electrical oscillations, especially the high-frequency oscillations above the fundamental frequency in large-scale power electronics based power systems like WPPs [52]. On the other hand, high-frequency oscillations in actual WPPs have frequently been reported. For example, in China, Shanxi province, electrical oscillations around 900 Hz was increased in a WPP and some equipment of the WTs

was broken [29]. Therefore, it is important to develop an effective approach to model and identify the electrical oscillations. After finding the main source of oscillations, its parameters can be redesigned or some active or passive filters may be added to guarantee the stability and reliability of WPPs. Therefore, the motivation of the project can be summarized as illustrated in Figure 1. 6. First, an effective approach should be presented to model and analyze the electrical oscillations around and above the fundamental frequency for different conditions. Then, improvements, optimization, participation factor analysis, and active damping methods should be carried out to damp the oscillations. The electrical oscillations in a WPP may be increased for two issues: Dynamic instability or grid disturbance amplification by resonances of the WPP. These two issues will be discussed in this thesis.

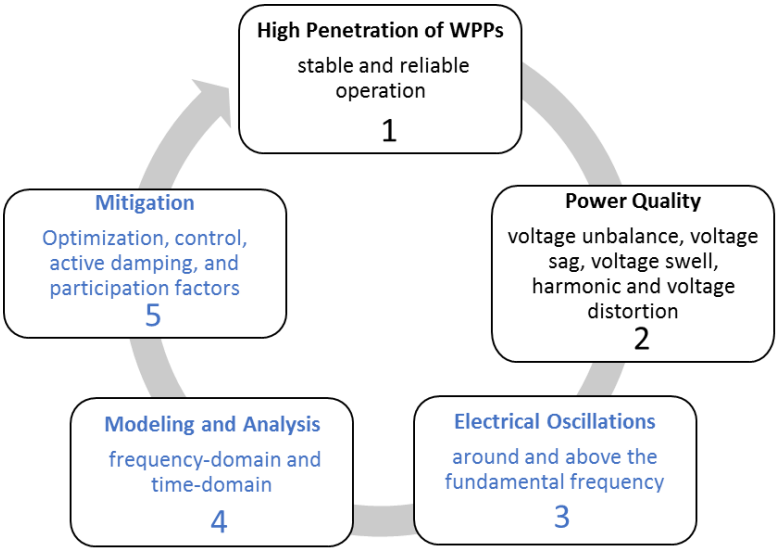

Figure 1. 6: Motivation of the project.

1.3.1. RESONANCES

If the dynamics of the power converters are neglected, a WT can be modelled as a ideal current source [53]-[55]. In this case, electrical resonances are originally coming from the interactions between the inductive and capacitive elements of the system like shown in Figure 1. 7.

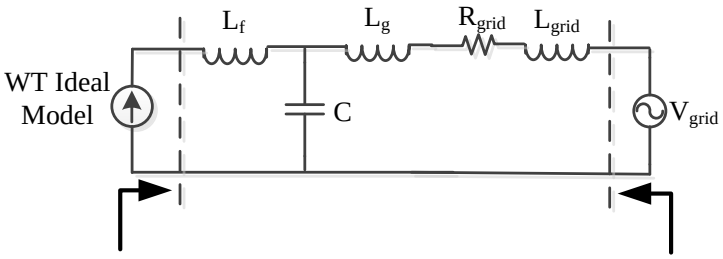

Figure 1. 7: Electrical resonances coming from passive components.

A lot of articles about harmonic resonance problems in WPPs have discussed such resonances coming from the passive components [56], [57]. However, besides the passive elements, the control loops of grid-connected power converters can present a capacitive or inductive behavior in various frequencies and thereby cause instability [58]. In Figure 1. 8, a grid-connected converter, which is shown in Figure 1.4, is modelled as a current source with a parallel active admittance (Y_f) [59].

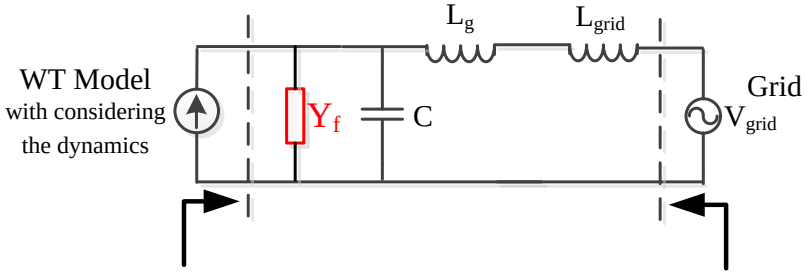

Figure 1. 8: Grid-connected power converter and its Norton equivalent model.

In a WPP, the interactions between these active admittances and passive admittances can create new resonances at different frequencies [60]-[62] as shown in Figure 1. 9.

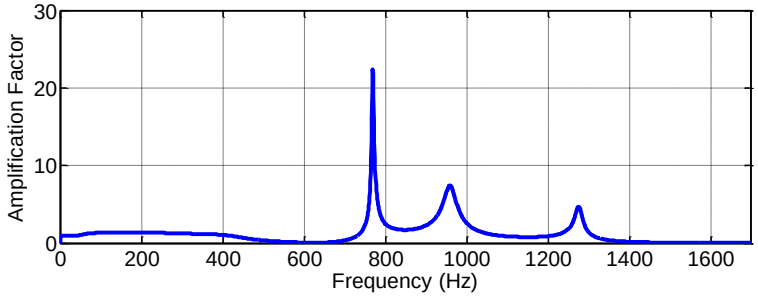

Figure 1. 9: Resonance characteristics in a Wind Power Plant (WPP)

On the other hand, as the amount of the non-linear loads is increasing, the power

grid voltage can be distorted. These harmonic emissions of the power grid can be amplified by the mentioned resonances of the WPPs [63].

1.3.2. INSTABILITY

As it is shown in Figure 1. 8, a grid-connected converter can be modelled by the Norton equivalent circuit around an operation point (small-signal modeling). The output admittance of the power converter (see Figure 1.8) in some frequency ranges can show a negative resistive behavior [64]. In a WPP, the interactions between these negative resistors and passive components can lead to an undesired dynamic response and even instability [65]-[68]. For the unstable cases, the magnitudes of some oscillations are increasing in the WPP until saturation occurs in the power system. This saturation usually will take place by the modulation index and the control loop output limiters of power electronic converters [69]. These electrical oscillations with various frequencies, coming from the power electronic converter dynamics, can be called harmonic instability [70].

1.4. ANALYSIS TOOLS

As it was mentioned, unexcepted electrical oscillations, which lead to instability and power quality problems, have been reported often in renewable energy systems. Therefore, it is important to present effective tools for modeling, predicting and mitigating these oscillations. In literature, time-domain analysis, frequency-domain analysis, participation factor analysis, aggregation method, and harmonic power flow method, have been presented to analyze power electronics based power systems [71].

1.4.1. NON-LINEAR TIME-DOMAIN ANALYSIS

Non-linear time-domain analysis is one of the effective ways to identify the instantaneous response of the system components for both electromagnetic and electromechanical systems [72]. PSCAD/EMTDC and RTDS are two popular time-domain approaches for power electronics based systems, where the differential equations of the power system are solved in every fixed time step [73].

- ✓ **PSCAD/EMTDC**

Non-linear time-domain simulations in the well-know software like PSCAD/EMTDC is a powerful tool for the detailed modeling and analysis of electrical oscillations and transients in the power system [74]. As the PSCAD software has the standard modules of the power system components, control blocks, and the power electronic switches, it is quite easy to simulate a power electronics based power system. In the numerical time-domain simulations, the resonance analysis and the impedance spectrum seen from a bus are determined by injecting a perturbation in the system [57]. As just one frequency can be identified during a simulation run, the

computational burden is high to identify the harmonic impedance in a frequency range with high resolution, especially for large-scale power electronics based power systems like WPPs [53].

- ✓ **RTDS**

Real Time Digital Simulator (RTDS) allows to test a power electronics based power system in the real time. The RTDS makes possible to analyze some physical equipment (like power converters and generators) within a simulated model of a large power system [73]. Therefore, the impact of the distributed generation systems in a power system with a high penetration of power converters can be analyzed for a more realistic condition and in the real time [75]. In recent years, RTDS simulations has been widely used to analyze the wind power plants [76], [77].

1.4.2. LINEARIZED FREQUENCY-DOMAIN ANALYSIS

Linearized frequency-domain analysis is accurate in the intended frequency range around an operation point but it has much lower computational burden than non-linear time-domain simulations [71]. In the frequency-domain, the electrical oscillations are identified based on the oscillatory modes of the system [78]. If any modes of the power system has a positive real part in an operation point, it shows that the system can not work in that operating point and the amplitudes of some harmonics are increased until the system is saturated because of any non-linear behavior of the system components [63], [64]. The state-space based analysis and the impedance-based analysis are two general approaches to analyze the system in the frequency-domain [65].

1.4.2.1 State-space based analysis

- ✓ **State-space averaging method**

State-space averaging modelling is a powerful tool to analyze the dynamic behavior of a system. A linear system is generally presented by the state-space method as:

$$\begin{aligned} \frac{d}{dt}x(t) = \dot{x}(t) &= A(t)x(t) + B(t)u(t) \\ y(t) &= C(t)x(t) + D(t)u(t) \end{aligned} \tag{1.3}$$

where *x*, *y*, and *u* are the state vector, the output vector, and the input vector, respectively. A, B, C, and D are the state matrix, input matrix, output matrix, and feedforward matrix, respectively [78]. This method can identify the contributions of every parameter of the system to the stability [79]. The state-space modeling has been done in different power electronics based power systems like microgrids, current source converters, and parallel voltage source inverters [80]- [82]. However, as the state-space method needs the information of each component of the dynamic system in details, it can be can be complex for large-scale power electronic systems like WPPs

[83]- [85].

- ✓ **Harmonic State-Space (HSS) method**

Harmonic State-Space (HSS) method is a useful methodology to analyze the Linear Time-Periodic (LTP) systems, where the frequency-coupling dynamics and oscillations can be identified [86]. The HSS model of a LTP system can be obtained by

$$\begin{aligned}(s+jk\omega_s)X_k(s)&=\sum_n A_{k-n}X_n(s)+\sum_n B_{k-n}U_n(s)\\ Y_k(s)&=\sum_n C_{k-n}X_n(s)+\sum_n D_{k-n}U_n(s)\end{aligned} \tag{1.4}$$

where A_k, B_k, C_k, and D_k are the Fourier coefficients of the A(t), B(t), C(t), and D(t), respectively [87]. HSS analysis is more accurate, compared to the state-space averaging method, for power electronic applications but it is more complex and needs more computational effort [87].

- ✓ **Component Connection Method (CCM)**

In Component Connection Method (CCM), first the power system is divided into different subsystems and each subsystem is modeled based on the state-space method as

$$\begin{aligned}\dot{x}_i&=A_i x_i+B_i u_i\\ y_i&=C_i x_i+D_i u_i\end{aligned} \tag{1.5}$$

where A_i, B_i, C_i, D_i are the state matrices, and x_i, u_i, y_i are the state variables, input and output variables for the i^{th} subsystem, respectively. Then, the all individual matrices will be located in the new diagonal matrices, which can be written as:

$$\begin{aligned}&A_i=diag\left(A_{i1}\ldots A_{ij}\right),\ B_i=diag\left(B_{i1}\ldots B_{ij}\right),\\ &C_i=diag\left(C_{i1}\ldots C_{ij}\right),D_i=diag\left(D_{i1}\ldots D_{ij}\right)\end{aligned} \tag{1.6}$$

The new state, input, and output variables of the system will be written as $x=[x_{11}\ldots x_{1j}]^T$, $u=[u_{11}\ldots u_{1j}]^T$, $y=[y_{11}\ldots y_{1j}]^T$. The final interconnection relationship between the all subsystems can be obtained by

$$\begin{aligned}u&=L_1 y+L_2 a\\ b&=L_3 y+L_4 a\end{aligned} \tag{1.7}$$

where a and b are the inputs and output vectors, and L_1 , L_2 , L_3 , and L_4 are the interconnection matrices [88]. By combining (1.5) to (1.7), the state-space modeling of whole system can be obtained by

$$\begin{aligned} \dot{x} &= F_T x + G_T a \\ b &= H_T x + J_T a \end{aligned} \tag{1.8}$$

The eigenvalues of the state matrix F_T can show the electrical modes of the power system. The CCM is much more systematic and modular for large power electronic systems, compared to the basic state-space averaging method [87]. The CCM is first presented for the dynamic stability of AC/DC power systems in [89]. It has been then applied in inverter-fed power system [88] and offshore WPPs for electrical oscillations analysis [78].

1.4.2.2 Impedance based analysis

Another powerful tool, for analysis of the dynamic system, is the impedance-based modeling, where the equivalent impedance ratios seen from the PCC are required. In this approach, the source output impedance (Z_s) and the load input impedance (Z_l) are obtained and then the interconnected system stability is assessed by the Nyquist criterion of the ratio of $Z_l(s)/Z_s(s)$ [90]. The impedance-based analysis can not identify the contributions of each parameter of a large-scale system to the instability [69]. The impedance-based analysis can be performed in the dq, sequence, or phasor domains [91].

- ✓ **Sequence domain**

When a three-phase balanced power converter is perturbed by injecting a disturbance at a frequency f_p, harmonic frequencies at $mf_p \pm nf_1$ in the output currents and voltages can be seen, where f_1 is the fundamental frequency [92], [93]. In a three-phase balanced system, the harmonic frequencies are dominated by frequency of f_p+f_1 in the positive sequence and frequency of $f_p - f_1$ in the negative sequence [94]. Therefore, by ignoring the other frequency components, the output voltage of the converter can be written as:

$$v_a = V_1 \cos(2\pi f_1 t + \phi_{v1}) + \hat{v}_p \cos\left[2\pi(f_p + f_1)t + \phi_{vp}\right] + \hat{v}_n \cos\left[2\pi(f_p - f_1)t + \phi_{vn}\right] \tag{1.9}$$

Fundamental positive-sequence component f1

Perturbation in positive-sequence $v_p = \hat{v}_p e^{j\phi_{vp}}$ *at* $f_p + f_1$

Perturbation in negative-sequence $v_n = \hat{v}_n e^{j\phi_{vn}}$ *at* $f_p - f_1$

By presenting the output current of the converter in the similar form of Equation (1.9), the small-signal relationship between the output current and voltages can be obtained by an impedance/admittance matrix [65] in the sequence domain as

$$\begin{bmatrix} v_p(s_p + j\omega_1) \\ v_n(s_n - j\omega_1) \end{bmatrix} = \begin{bmatrix} z_{pp}(s) & z_{pn}(s) \\ z_{np}(s) & z_{nn}(s) \end{bmatrix} \begin{bmatrix} i_p(s_p + j\omega_1) \\ i_n(s_n - j\omega_1) \end{bmatrix}$$

$$\begin{bmatrix} i_p(s_p + j\omega_1) \\ i_n(s_n - j\omega_1) \end{bmatrix} = \begin{bmatrix} y_{pp}(s) & y_{pn}(s) \\ y_{np}(s) & y_{nn}(s) \end{bmatrix} \begin{bmatrix} v_p(s_p + j\omega_1) \\ v_n(s_n - j\omega_1) \end{bmatrix} \quad (1.10)$$

- ✓ **DQ domain**

There-phase variables like Equation (1.9) can be transformed into the dq domain by the Park's transformation, i.e.,

$$\begin{bmatrix} x_d \\ x_q \end{bmatrix} = \frac{2}{3} \begin{bmatrix} \cos(\theta) & \cos(\theta - \frac{2\pi}{3}) & \cos(\theta + \frac{2\pi}{3}) \\ -\sin(\theta) & -\sin(\theta + \frac{2\pi}{3}) & -\sin(\theta + \frac{2\pi}{3}) \end{bmatrix} \begin{bmatrix} x_a \\ x_b \\ x_c \end{bmatrix} \quad (1.11)$$

By applying some trigonometric formulas and simplification, the small-signal impedance/admittance of a three-phase converter can be obtained in the dq-domain [84], [95] by

$$\begin{bmatrix} v_d(s_{dq}) \\ v_q(s_{dq}) \end{bmatrix} = \begin{bmatrix} z_{dd}(s) & z_{dq}(s) \\ z_{qd}(s) & z_{qq}(s) \end{bmatrix} \begin{bmatrix} i_d(s_{dq}) \\ i_q(s_{dq}) \end{bmatrix}$$

$$\begin{bmatrix} i_d(s_{dq}) \\ i_q(s_{dq}) \end{bmatrix} = \begin{bmatrix} y_{dd}(s) & y_{dq}(s) \\ y_{qd}(s) & y_{qq}(s) \end{bmatrix} \begin{bmatrix} v_d(s_{dq}) \\ v_q(s_{dq}) \end{bmatrix} \quad (1.12)$$

The relationship between the sequence-domain admittance definition and the dq-domain admittance definition can be obtained [96] by

$$\begin{bmatrix} y_{pp}(s) & y_{pn}(s) \\ y_{np}(s) & y_{nn}(s) \end{bmatrix} = \begin{bmatrix} 1 & 1 \\ -j & j \end{bmatrix}^{-1} \begin{bmatrix} y_{dd}(s) & y_{dq}(s) \\ y_{qd}(s) & y_{qq}(s) \end{bmatrix} \begin{bmatrix} 1 & 1 \\ -j & j \end{bmatrix} \quad (1.13)$$

- ✓ **Phasor domain**

In power systems, three-phase currents and voltages are usually presented by their dynamic phasor definitions. By injecting the perturbation in the magnitude and the phase angle of the fundamental-frequency phasors, the impedance matrix of the converter can be defined [91] as

$$\begin{bmatrix} \hat{V}_m(s_{m\theta}) \\ \theta_V(s_{m\theta}) \end{bmatrix} = \begin{bmatrix} z_{dd}(s) & z_{dq}(s) \\ z_{qd}(s) & z_{qq}(s) \end{bmatrix} \begin{bmatrix} \hat{I}_m(s_{m\theta}) \\ \theta_I(s_{m\theta}) \end{bmatrix}$$

$$\begin{bmatrix} \hat{I}_m(s_{m\theta}) \\ \theta_I(s_{m\theta}) \end{bmatrix} = \begin{bmatrix} y_{dd}(s) & y_{dq}(s) \\ y_{qd}(s) & y_{qq}(s) \end{bmatrix} \begin{bmatrix} \hat{V}_m(s_{m\theta}) \\ \theta_V(s_{m\theta}) \end{bmatrix} \quad (1.14)$$

1.4.3. PARTICIPATION FACTOR ANALYSIS

Participation Factor (PF) analysis is a useful methodology to identify the critical modes of the interactions between different components of the wind power system [97]. In this approach, the parameter sensitivity to system variations is obtained to identify how the controller parameters of the wind turbines should be modified, in order to improve the overall system stability and dynamic behavior [98]. PF analysis specifies which component of the system has a higher participation in the electrical oscillations, or at which buses the electrical oscillations can be observed or controlled [99]. PF analysis can be performed in both time-domain and frequency-domain. In the frequency-domain, the PF of sate variables are calculated based on the eigenvectors of the state matrix [100], [101]. However, the impedance-based analysis is not able to identify the PF contribution of the system parameters to electrical oscillations [98].

1.4.4. AGGREGATION METHOD

For a very large WPP, it is not possible to simulate and model all individual WTs in details. For example, in [102], the stability of a WPP including 136 WTs is analyzed, where all individual WTs are considered. In this case, 3436 differential equations are solved for the time-domain analysis, and 2546 eigenvalues are obtained for the linearized frequency-domain analysis. Therefore, the analysis of such a system is not so practical. In order to simplify a large WPP, where a lot of WTs, passive filters, cables, and transformers are located, an aggregated model of the WPP may be used [85], [9]. In the aggregated model, it is assumed that the wind speed across the WPP is constant and the WTs operate under the nominal conditions [58]. Aggregation methods can identify the overall behavior of the WPP from the Point of Common Coupling (PCC) but some internal resonant modes may be eliminated and thereby the accuracy of the method becomes limited [103].

1.4.5. HARMONIC POWER FLOW METHOD

Harmonic power flow method is a general tool to assess the harmonics of the power system in the steady-state conditions. In this approach, every component of the system is modeled by a function as

$$(I_1, I_2, ..., I_h) = F_h(V_1, V_2, ..., V_h, C_1, C_2, ..., C_m) \quad (1.15)$$

where (I_1, I_1, …, I_h) are the current harmonics, (V_1, V_1, …, V_h) are the voltage harmonics, and (C_1, C_1, …, C_m) are the control parameters [104]. The non-linear equation is solved by Newton type algorithms for all harmonic orders. Harmonic power flow analysis is a powerful tool for the steady-state harmonics [105]. Harmonic power flow makes possible to analyze the distribution systems for a very unbalanced conditions [104] and power sharing [105]. However, this method can not assess the dynamic oscillations, resulting from the time-varying factors or dynamic interactions between the power electronic converters [106].

1.4.6. COMPARISON OF ANALYSIS TOOLS

Table 1. 2 compares the analysis tools, including the basic state-space averaging method, HSS, CCM, impedance-based analysis, aggregation method, and harmonic power flow method, for different features. The HSS model and the harmonic power flow methods are more accurate than other methods, but they need more computational efforts [71]. The basic state-space modeling and the CCM are useful to identify the dynamic oscillatory modes of the system. The impedance-based analysis is an attractive methodology for the black-box modeling, where the detailed information of the converter is not available [109]. However, both state-space averaging modeling and impedance-based analysis are not so useful for the unbalanced grid conditions [65]. The superior feature of the aggregation method is to model large power systems with a low computational burden, and can be scalable and modular to different scales of the power systems [87]. The state-space averaging method and the CCM provide a good design-oriented analysis by calculating the participation factors of the state variables for different conditions [102]. As it can be seen, the HSS method is the most efficient method to analyze the frequency-coupling dynamics of the power system [86].

Table 1. 2: Comparison of analysis tools for different features.

Features	Basic state space averaging method	Harmonic State-Space (HSS) method	Component Connection Method (CCM)	Impedance-based analysis	Aggregation method	Harmonic power flow method
Accuracy	+++	++++	+++	+++	++	++++
Simple and Less computational burden	+++	++	+++	+++	++++	++
Oscillatory mode identification	++++	+++	++++	++	++	+
Unbalanced conditions	+	++++	+	+	+	+++
Frequency-coupling dynamics	++	++++	++	+++	+	+
Design-oriented analysis	++++	++	++++	+++	++	+
Black-box modeling	+++	+++	+++	++++	++++	+
Modularity	++	+	+++	++++	++++	++

1.5. PROJECT OBJECTIVES

With increasing the number of Wind Turbines (WTs) and Wind Power Plants (WPPs) in the power grid, the electrical oscillations and harmonic issues are becoming more and more important. Consequently, this project is defined to discuss various aspects related to the electrical oscillations in WPPs, including modeling, analysis, control, design, and optimization. Based on some assumptions, the main objective of this PhD project is to answer the following questions:

- Is it possible to model and predict the electrical oscillations and resonances in a WPP by a mathematical model based analytical tool?

The first task of this PhD project is to focus on a comprehensive modeling of large WPPs in the frequency-domain to analyze the electrical oscillations coming from the interactions between the power electronic converter dynamics and passive components.

- What are the effects of the number of WTs, Short Circuit Ratio (SCR), lengths of the power cables, and the bandwidths of the control loops on the electrical oscillations in a WPP?

In the second task, in a WPP, the number of WTs, the SCR of the power grid, cable lengths, and control loop bandwidths are increased or decreased to analyze their

effects on the electrical oscillations.

- Is it possible to find the main source of electrical oscillations in a WPP? Where is the most suitable location to install active or passive damping devices to reduce the oscillations?

In the third task, sensitivity analysis is performed to locate which parts have most contribution in harmonic-frequency oscillations and which bus excites the resonances more than others.

- How can the electrical oscillations be damped and mitigated in a WPP? Is it possible to find a design procedure for WTs to reduce the electrical oscillations and guarantee the dynamic performance of the WPP?

Last but not least, the grid-connected power converter parameters should be redesigned by an optimization procedure in order to guarantee the stable operation and dynamic response of the whole WPP.

1.6. 400-MW WIND POWER PLANT AS A CASE STUDY

In this project, a 400-MW WPP with four aggregated strings is tested as a case study [107], where its schematic is shown in Figure 1. 10.

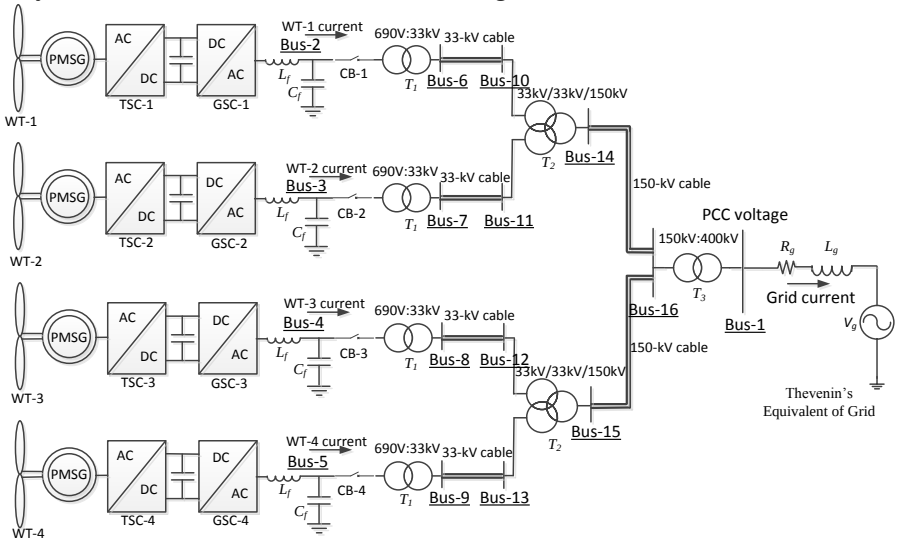

Figure 1. 10: 400-MW Wind Power Plant (WPP) with aggregated strings which is used as a case study in this project.

Every string is equivalent to fifteen WTs of 6.7 MW as shown in Figure 1. 11. As it can be seen, every string is divided into three radial feeders, where five WTs are installed on each radial feeder. Three radial feeders have the same structure and they

are connected in parallel to the same collector. Therefore, the total capacity of each feeder is 33 MW and each string is 100 MW. For nominal conditions, as the number of WTs is increasing, the feeder current is increasing towards the collector bus. Therefore, a cable which is closer to the collector bus should have larger cross-section than a cable which is further away from the grid. Consequently, on each feeder, the cables with different cross-sections (95 mm^2, 240 mm^2, and 400 mm^2) are considered.

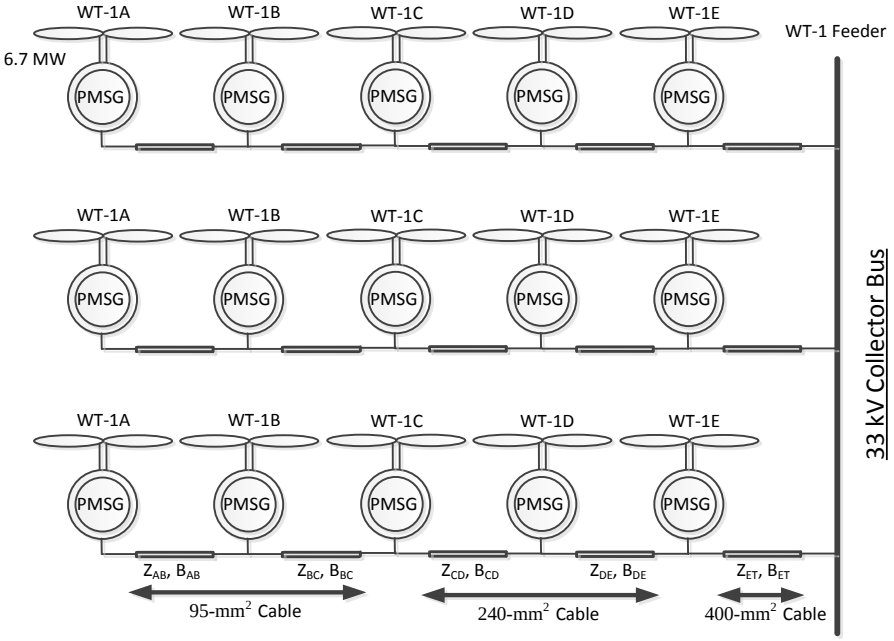

Figure 1. 11: Installed Wind Turbines (WTs) on each string of the Wind Power Plant (WPP) shown in Figure 1. 10.

Five 6.7-MW WTs of each feeder can be aggregated by one 33-MW WT as shown in Figure 1. 12. By assuming that the injected currents of the WTs on a feeder are the same, and the voltages have the nominal magnitudes for the normal conditions, the equivalent impedance parameters of a 33-MW WT can be obtained by

$$Z_{AT} = \frac{Z_{AB} + 4Z_{BC} + 9Z_{CD} + 16Z_{DE} + 25Z_{ET}}{25}$$
$$B_{AT} = B_{AB} + B_{BC} + B_{CD} + B_{DE} + B_{ET} \quad (1.16)$$

where, Z_{AT} and B_{AT} are the equivalent series impedance and the equivalent shunt susceptance, respectively. Z_{AB}, Z_{BC}, Z_{CD}, Z_{DE}, and Z_{ET} are the series impedances of the sections and B_{AB}, B_{BC}, B_{CD}, B_{DE}, and B_{ET} are the shunt susceptances (see Figure 1. 11). Finally, the 33.3-MW aggregated wind turbines on three parallel feeders can be aggregated as one 100-MW wind turbine (see Figure 1. 12). The equivalent series impedance and shunt susceptance can be calculated by

$$Z_{33} = \frac{Z_{AT}}{3} \qquad B_{33} = 3B_{AT} \tag{1.17}$$

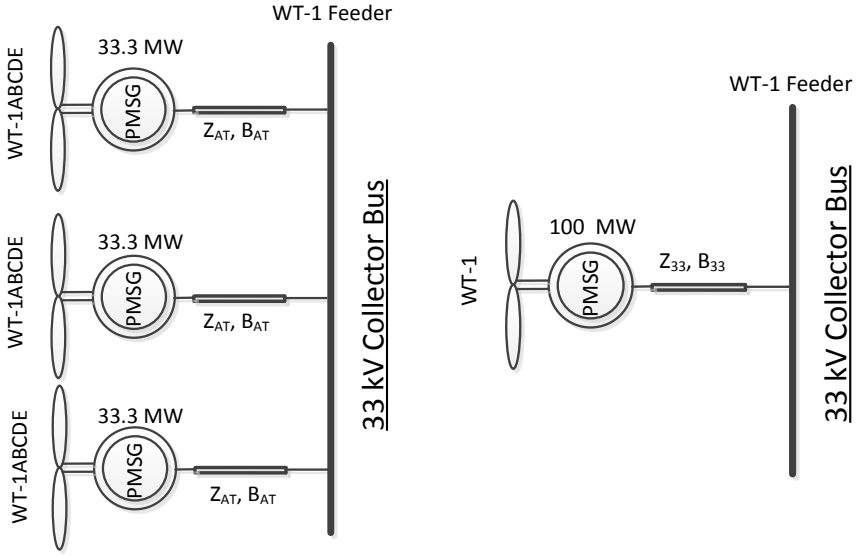

(a) aggregated model on each feeder (b) aggregated model of three feeders

Figure 1. 12: Aggregated model of the 15 Wind Turbines (WTs) shown in Figure 1. 11.

1.7. LIMITATIONS

In this thesis, as the grid is assumed to be a three-phase balanced system, the positive-sequence impedances are considered for each phase. The grid is also modelled as a simple Thévenin's equivalent circuit.

A PMSG-based WPP with full-scale power converters are studied. However, the proposed analysis and development methodologies can be applied to every power electronics based power system like DFIG-based WPPs, PV systems, HVDC, etc.

Many power electronic researchers have already discussed about the switching harmonics of the power electronic devices, which are in a few kilo hertz range [93]. On the other hand, many power system researchers have paid attention to the electromechanical oscillations related to the generator's shaft, which are in the Hertz range [50], [51]. Therefore, both mentioned frequency ranges, i.e., very low frequencies or very high frequencies, are not the scope and purpose of this project.

However, this project focuses on the oscillations between these two ranges, i.e., around the frequency of the fundamental component of the grid voltage (50 Hz) until around half of the switching frequency.

1.8. THESIS OUTLINE

The results and the contributions of the project, including modelling, control, design, and optimization, are summarized in this PhD thesis, which is organized in four chapters as follows:

In Chapter 1, the background and challenges of the project is briefly introduced. The important and some reasons of electrical oscillations in WPPs are investigated. It is also mentioned that electrical oscillations can be divided into two categories: grid disturbance amplification by resonances and harmonic instability coming from the interactions between the power converter dynamics and passive components.

In Chapter 2, a modeling and analysis methodology in the frequency-domain is proposed, as the non-linear time-domain simulations analysis has a high computational burden for large WPPs. The effect of system variations like the number of WTs, grid SCR, cable lengths, and controller bandwidths are analyzed. After finding the unstable conditions, design of some active damping controllers are discussed to stabilize the WPP.

In Chapter 3, sensitivity analysis and Participation Factor (PF) analysis are applied based on the proposed model in the frequency-domain. PF analysis locates which parts have more contribution in the oscillations and which bus excites the resonances more. It is discussed that the oscillations can be reduced by removing or redesigning a component with the largest PF.

Chapter 4 investigates the design of WTs for the ideal grid, which cannot guarantee the stable operation of whole WPP. Therefore, in order to damp and to reduce the oscillations, a multi-objective optimization procedure is employed to redesign the parameters of the WT controllers.

In Chapter 5, the overall conclusions of the project and the main contributions of the thesis are summarized, as well as some possible future works are given.

CHAPTER 2. MODELING AND ANALYSIS

2.1. ABSTRACT

This chapter presents a mathematical model based analytical tool for analyzing the electrical oscillations in WPPs, where the linearized frequency-domain models of the power converters are considered. Based on some assumptions, a WPP is introduced as Multi-Input Multi-Output (MIMO) control system. The oscillatory modes of the WPP are calculated based on the MIMO transfer function matrix. Besides, the resonances are identified by the magnitudes of the MIMO matrix elements. Various case studies show that the number of WTs, the grid SCR variations, cable lengths, and the controller bandwidths can affect the stability. The effectiveness of the proposed modelling is verified by time-domain simulations of the 400-MW WPP using the PSCAD software.

2.2. PROPOSED METHOD FOR MODELING AND ANALYSIS

The conventional method for doing electrical oscillation analysis of power systems is the state-space modeling, where the oscillations are assessed based on the eigenvalues of the state-space matrix. So far, the state-space modeling has been done in different power electronics based power systems like microgrids, current source converters, and paralleled voltage source inverters [79]-[82]. However, as the state-space method requires detailed models of each component, it can be complex for large-scale power electronic systems like large WPP [83]-[85]. Another powerful method is the impedance based analysis, where the equivalent impedance seen from Point of Connection (PoC) are required. The impedance based analysis has also been done in some power electronic systems like parallel power electronic converters, and voltage source inverters in the current-control mode and in the voltage-control mode [86]-[88]. However, this method can not identify which bus in a power electronics based system has more contributions to the electrical oscillations. Therefore, in this chapter, a general approach to model the electrical oscillations of WPPs is proposed, which is simple to apply in large-scale power systems and it is able to identify the main source of the oscillations.

In the proposed model, every component of the WPP, including the WTs and passive components, are modeled as Norton equivalent circuits in the s-domain:

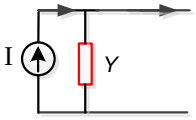

Figure 2. 1: Norton equivalent circuit for every component of the Wind Power Plant (WPP).

After that, the relationships between the equivalent current sources and the bus voltages of the WPP can be written by the nodal admittance matrix as

$$\begin{bmatrix} I_g \\ I_{c-1} \\ I_{c-2} \\ \vdots \\ I_{c-n} \\ 0 \\ \vdots \\ 0 \end{bmatrix} = \begin{bmatrix} Y_{11} & -Y_{12} & -Y_{13} & \cdots & -Y_{1(n+1)} & -Y_{1(n+2)} & \cdots & -Y_{1m} \\ -Y_{21} & Y_{22}+Y_{c-1} & -Y_{23} & \cdots & -Y_{2(n+1)} & -Y_{2(n+2)} & \cdots & -Y_{2m} \\ -Y_{31} & -Y_{32} & Y_{33}+Y_{c-2} & \cdots & -Y_{3(n+1)} & -Y_{3(n+2)} & \cdots & -Y_{3m} \\ \vdots & \vdots & \vdots & \vdots & \vdots & \vdots & \vdots & \vdots \\ -Y_{(n+1)1} & -Y_{(n+1)2} & -Y_{(n+1)3} & \cdots & Y_{(n+1)(n+1)}+Y_{c-n} & Y_{(n+1)(n+2)} & \cdots & -Y_{(n+1)m} \\ -Y_{(n+2)1} & -Y_{(n+2)2} & -Y_{(n+2)3} & \cdots & -Y_{(n+2)(n+1)} & Y_{(n+2)(n+2)} & \cdots & -Y_{(n+2)m} \\ \vdots & \vdots & \vdots & \vdots & \vdots & \vdots & \vdots & \vdots \\ -Y_{m1} & -Y_{m2} & -Y_{m3} & \cdots & -Y_{mn} & -Y_{m(n+2)} & \cdots & Y_{mm} \end{bmatrix} \begin{bmatrix} V_1 \\ V_2 \\ V_3 \\ \vdots \\ V_n \\ V_{(n+1)} \\ \vdots \\ V_m \end{bmatrix} \tag{2.1}$$

where it is assumed that bus *1* is the main power grid and bus *2* to bus *n+1* are WTs busses. $Y_{c\text{-}k}$ *(k=1,2, …,n)* is the equivalent active admittance of the k^{th} WT, Y_{ii} is the passive admittance connected to the i^{th} bus, $Y_{ij}(s)$ *(i,j=1,2, …,m, and i≠j)* is the admittance between the i^{th} bus and the j^{th} bus. Equation (2.1) can be written as

$$\mathbf{V(s) = G^{-1}(s)I(s)} \tag{2.2}$$

$\mathbf{G^{-1}(s)}$ in the above equation is in the s-domain and it is a MIMO transfer function matrix. The poles of the $\mathbf{G^{-1}(s)}$ can be calculated by

$$\det\left[\mathbf{G(s)}\right] = 0 \;\Rightarrow p_1 = \alpha_1 + \mathrm{j}\beta_1, p_2 = \alpha_2 + \mathrm{j}\beta_2, \cdots, p_q = \alpha_q + \mathrm{j}\beta_q \tag{2.3}$$

The poles of $\mathbf{G^{-1}(s)}$ are generally the poles of its elements. Therefore, an element of $\mathbf{G^{-1}(s)}$ in the s-domain can be written as

$$G_{ij}(s) = \frac{P(s)}{(s-p_1)(s-p_2)\cdots(s-p_q)} = \frac{A_1}{(s-p_1)} + \frac{A_2}{(s-p_2)} + \cdots + \frac{A_q}{(s-p_q)} \tag{2.4}$$

By applying the transform of the inverse Laplace, $G_{ij}(t)$ in the time-domain are obtained by

$$\begin{aligned} G_{ij}(t) &= A_1 e^{p_1 t} + A_2 e^{p_2 t} + \cdots + A_q e^{p_q t} \\ &= A_1 e^{\alpha_1 t} e^{j\beta_1 t} + A_2 e^{\alpha_2 t} e^{j\beta_2 t} + \cdots + A_q e^{\alpha_q t} e^{j\beta_q t} \end{aligned} \tag{2.5}$$

If one of the poles has a positive real part ($\alpha_q > 0$), $A_q e^{\alpha_q t} e^{j\beta_q t}$ in $G_{ij}(t)$ is a sinusoidal waveform with the frequency $\frac{\beta_i}{2\pi}$ Hz with an increasing exponential magnitude. Therefore, the poles of $G_{ij}(s)$ in the s-domain show the oscillations of $G_{ij}(t)$ in the time-domain. In order to have a stable system without electrical oscillations, all

poles should have negative real parts. In the following sections, more details about modeling of the WTs and the WPP, including the current controller and the Phase-Locked Loop (PLL), are given.

2.3. CURRENT CONTROLLER LOOP EFFECT

2.3.1. PAPER 1

Title: Harmonic stability and resonance analysis in large PMSG-based wind power plants

E. Ebrahimzadeh, F. Blaabjerg, X. Wang, and C. L. Bak
in IEEE Transactions on Sustainable Energy, vol. 9, no. 1, pp. 12-23, Jan. 2018.

✓ Contributions

- Presenting the WPP by a Multi-Input Multi-Output (MIMO) transfer function matrix in the frequency-domain
- Identifying the resonances, which leads to a grid harmonic background amplification
- Specifying the stability border of the WPP
- Analyzing of the effects of the number of WTs and the grid SCR on resonances and electrical oscillations
- Designing of the active damping controllers to improve the stability of the system

✓ Results

The number of the WTs in the aggregated 400-MW WPP, which is shown in Figure 1. 10 , is increased from one WT to four WTs. Table 2. 1 shows the corresponding results of the proposed frequency-domain analysis for different cases. As it can be seen, the real part of the critical pole is increasing to the positive values by increasing the number of the WTs. Case IV, where all four WTs are connected to the WPP, has a pole with a positive real part and thereby Case IV is an unstable case.

Table 2. 1: The critical pole of the 400-MW WPP for different cases.

Case	connected wind turbines in WPP	Pole	Frequency
I	WT-1	-129.5±4428.9i	705 Hz
II	WT-1 and WT-2	-74.03±4748.8i	756 Hz
III	WT-1, WT-2, and WT-3	-14.977±5068.2i	806 Hz
IV	WT-1, WT-2, WT-3, and WT-4	11.659±5267.1i	838 Hz

In order to validate these frequency-domain results, time-domain simulations in the PSCAD software have been performed in Figure 2. 2. In this figure, Case IV is changed to Case III at t = 0.5 s, i.e., WT-4 is disconnected form the WPP at t = 0.5 s. As it is predicted by the proposed frequency-domain analysis, the current waveforms in Case IV are unstable and oscillate a lot. However, Case III is a stable case with the pure sinusoidal waveforms.

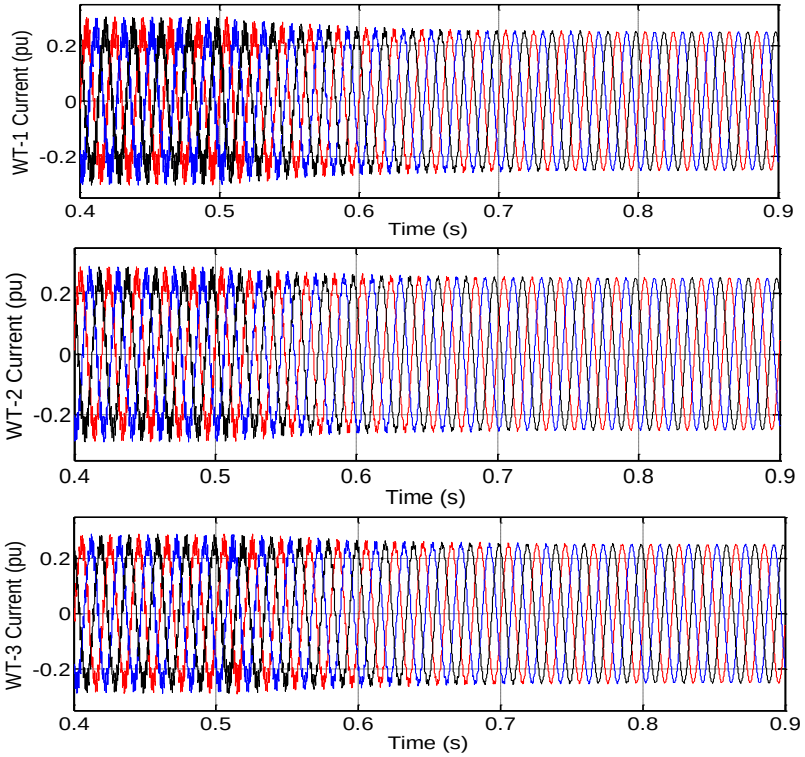

Figure 2. 2: Time-domain simulation results, where WT-4 is disconnected from the WPP at t = 0.5 s [83].

In Figure 2. 3, the FFT analysis has been performed for the WT-1 current waveform, which is shown in Figure 2. 2. The frequencies of oscillations are around 835 Hz and 805 Hz before t = 0. 5 s and after t = 0. 5 s, respectively. These results match the frequency of the critical pole in Table 2. 1.

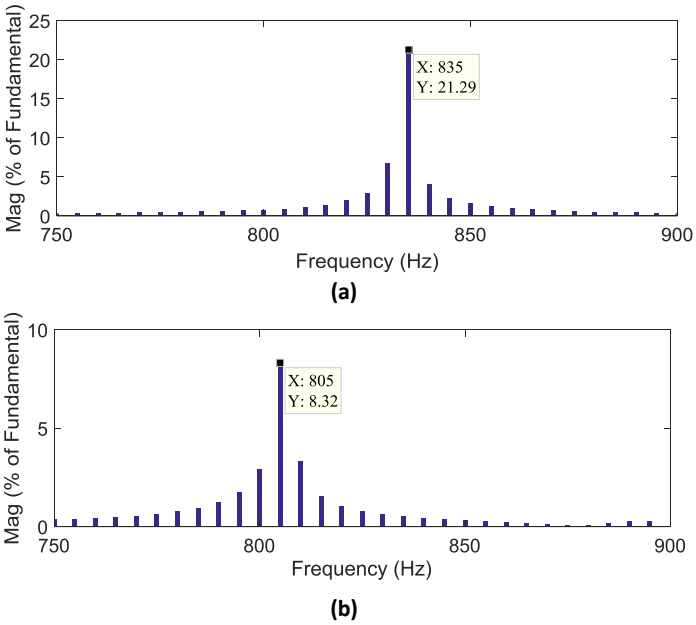

Figure 2. 3: FFT analysis of the WT-1 current, which is shown in Figure 2. 2, (a) before t = 0.5 s, (b) after t = 0.5 s [83].

2.4. GRID SYNCHRONIZATION LOOP EFFECT

2.4.1. PAPER 2

Title: Small signal modeling of wind farms

E. Ebrahimzadeh, F. Blaabjerg, X. Wang, C. L. Bak, T. Lund, G. K. Andersen, C. G. Suárez, and J. Berg
in Proc. of IEEE ECCE Conference, USA, 2017, pp. 1-7.

✓ **Contributions**

- ✓ Modeling of low-frequency oscillations coming from the interactions between the low-bandwidth control loops like Phase-Locked Loops (PLLs)
- ✓ Analyzing the effects of the PLL's bandwidth and the cable lengths on the electrical oscillations

✓ **Results**

The PLL bandwidths and cable lengths in the 400-MW WPP are increased from 30

Hz to 40 Hz, and 5 km to 25 km, respectively. Table 2. 2 shows the real part and the frequency of the critical mode of the WPP, which is obtained by the proposed frequency-domain analysis. As it can be seen, the real part of the critical pole is increasing to the positive values by increasing the PLL bandwidths and the cable lengths. As the frequencies of the unstable modes are around 100 Hz, low-frequency oscillations propagate into the WPP, resulting from the instability.

Table 2. 2: The critical pole of the 400-MW WPP for different PLL bandwidths and cable lengths.

PLL bandwidth and cable length	Real part	Frequency in dq-domain	Frequency in abc-domain
BWpll = 30 Hz, Lcable = 5 Km	-14.3013	133 Hz	183 Hz and 83 Hz
BWpll = 40 Hz, Lcable = 5 Km	4.83829	134 Hz	184 Hz and 84 Hz
BWpll = 30 Hz, Lcable = 25 Km	11.9659	113 Hz	163 Hz and 63 Hz

In order to confirm these frequency-domain results, the non-linear time-domain simulations have been carried out in the PSCAD software. In Figure 2. 4, the bandwidth of the PLL is increased from 30 Hz to 40 Hz at t = 3.2 s. As it is shown in Figure 2. 4, low-frequency electrical oscillations propagate into the WPP after t = 3.2 s, where the proposed frequency-domain results are also confirming these oscillations.

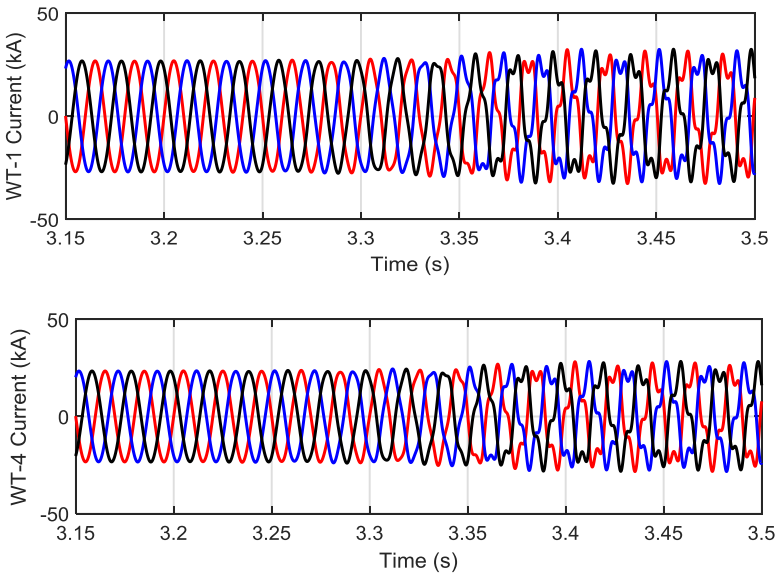

Figure 2. 4: WT-1 and WT-4 current waveforms, when the PLL bandwidth is increased from 30 Hz to 40 Hz at t = 3.2 s (L_{cable} = 5 km) [84].

Figure 2. 5 shows the WT-1 current waveform and its FFT analysis, where the cable

length has been increased (L_{cable} =25 km and BW_{PLL} = 30 Hz). As it can be seen, the oscillation frequencies are around 154 Hz and 54 Hz, which the obtained results in Table 2. 2 are sufficiently predicting these frequencies. The small error is resulting from the non-linearity behavior of the PLL and the WPP.

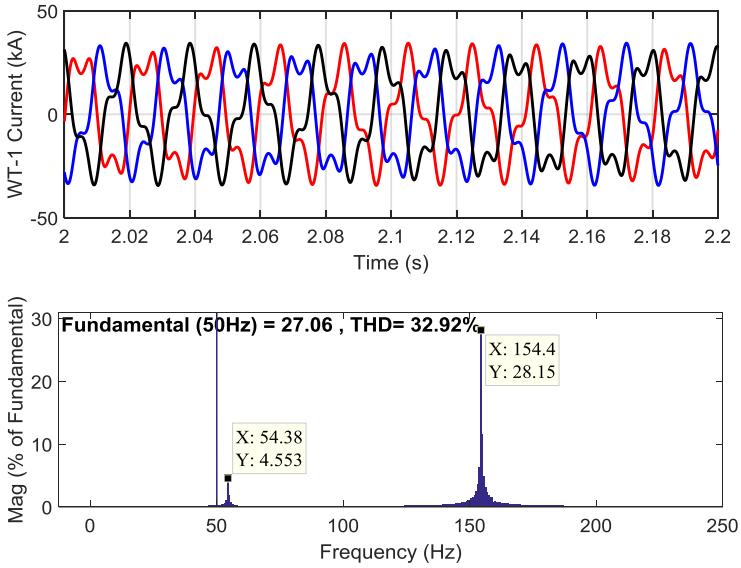

Figure 2. 5: WT-1 current waveform for the increased cable lengths (L_{cable} =25 km and BW_{PLL} = 30 Hz) [84].

CHAPTER 3. PARTICIPATION FACTOR AND SENSITIVITY ANALYSIS

3.1. ABSTRACT

In this chapter, by presenting a WPP as a Multi-Input Multi-Output (MIMO) transfer function matrix, sensitivity analysis can be performed and Participation Factors (PFs) of different buses for the oscillatory modes are calculated. PF analysis can identify which bus has more contributions to the electrical oscillations or which bus is the main source of resonances. Time-domain simulations show that disconnecting a WT with the largest PF leads to oscillations damping in the WPP. In addition, the simulation results show that a bus with a larger PF amplifies the harmonics more than the other buses.

3.2. PROPOSED METHOD FOR SENSITIVITY ANALYSIS

As it was discussed in the previous chapter, the oscillatory modes of the WPP can be identified by

$$\det\left[\mathbf{G(s)}\right]=0 \;\Rightarrow p_1=\alpha_1+\mathrm{j}\beta_1,\, p_2=\alpha_2+\mathrm{j}\beta_2,\cdots,\, p_q=\alpha_q+\mathrm{j}\beta_q \tag{3.1}$$

G (s) can be numerically obtained for each oscillatory mode (p_q) by substituting p_q with s. By applying the eigenvalue decomposition idea [108], [109], the matrix **G** (p_q) can be rewritten by multiplication of three different matrices as

$$\mathbf{G}(p_q)=\mathbf{R\Lambda L}=\mathbf{R}\begin{bmatrix}\lambda_1 & 0 & 0 & 0\\ 0 & \lambda_2 & 0 & 0\\ 0 & 0 & \cdots & 0\\ 0 & 0 & 0 & \lambda_m\end{bmatrix}\mathbf{L} \tag{3.2}$$

where **Λ** is a matrix, which its diagonal elements are the eigenvalues of **G** (p_q) (λ_1, λ_2, …, λ_m). **R** is a matrix where its columns are the right eigenvectors, i.e.,

$$\mathbf{G}(p_q)\mathbf{R}=\mathbf{R\Lambda} \tag{3.3}$$

L is a matrix where its rows are the left eigenvectors, i.e,

$$\mathbf{LG}(p_q) = \mathbf{\Lambda L} \tag{3.4}$$

It can be found from (3.3) and (3.4), Matrix **L** is equal to the inverse of Matrix **R**, i.e,

$$\mathbf{L} = \mathbf{R}^{-1} \tag{3.5}$$

Based on (3.2) and (3.5), the $\mathbf{G}(p_q)$ inverse are identified by

$$\mathbf{G}^{-1}(p_q) = \mathbf{R}\ \mathbf{\Lambda}^{-1}\mathbf{L}\ = \mathbf{R}\begin{bmatrix} 1/\lambda_1 & 0 & 0 & 0 \\ 0 & 1/\lambda_2 & 0 & 0 \\ 0 & 0 & \cdots & 0 \\ 0 & 0 & 0 & 1/\lambda_m \end{bmatrix}\mathbf{L} \tag{3.6}$$

As p_q is one of the poles of Matrix $\mathbf{G^{-1}(s)}$, one eigenvalue of $\mathbf{G}(p_q)$ ($\lambda_1, \lambda_2, \ldots,$ or λ_m) would be very small close to zero. If λ_c is the i^{th} eigenvalue, the right eigenvector ($\mathbf{r_c}$) of this eigenvalue (λ_c) is the i^{th} column of Matrix **R** and the left eigenvector ($\mathbf{l_c}$) is the i^{th} row of Matrix **L**. If the right eigenvector ($\mathbf{r_c}$) is multiplied by the left eigenvector ($\mathbf{l_c}$), Matrix $\mathbf{S_{\lambda c}}$ is obtained, whose diagonal elements show the PFs and the sensitivity of different busses for the critical mode (p_q).

$$\mathbf{S}_{\lambda c} = \frac{\partial \lambda_c}{\partial\left[\mathbf{G}(p_q)\right]} = \mathbf{r_c l_c} \tag{3.7}$$

If the k^{th} diagonal element of Matrix $\mathbf{S_{\lambda c}}$ is the largest element for an oscillatory or resonance mode, it will mean that the k^{th} bus in the WPP is the main source of the oscillations or resonance, where it is also the best place to install active or passive damping. In the following sections, the proposed methodology is discussed in details along with time-domain simulation results.

3.3. BUS PARTICIPATION FACTOR ANALYSIS FOR OSCILLATORY MODES

3.3.1. PAPER 3

Title: Bus participation factor analysis for harmonic instability in power electronics based power systems

E. Ebrahimzadeh, F. Blaabjerg, X. Wang, and C. L. Bak,
IEEE Transactions on Power Electronics, 2018, early access

✓ Contributions

- Identifying which bus has more contribution in the oscillations and which WT is the main source of the oscillations
- Reducing the oscillations by removing or redesigning a component with the largest participation factor

✓ Results

In this paper, the GSC parameters of the WTs are designed different form each other but with the acceptable bandwidths. In this case, the 400-MW WPP has an unstable mode with frequency of 839.9 Hz. In order to identify the main source of this oscillatory mode, the proposed PF analysis approach has been performed in Table 3. 1. As it can be seen, Bus-5 (WT-4) has the largest PF, while other buses have a very small PF for the unstable mode. Therefore, in this case, WT-4 can be the most influencing WT for the electrical oscillations.

Table 3. 1: Participation Factor (PF) analysis for the unstable mode.

Bus number	PF for the unstable mode (P_9=20.587±5277.43i)
Bus-2 (WT-1)	0.1095e-1
Bus-3 (WT -2)	0.346e-3
Bus-4 (WT -3)	0.128e-3
Bus-5 (WT -4)	0.737738

The corresponding time-domain analysis has been done in Figure 3. 1 by simulating the 400-MW WPP in the PSCAD software. Figure 3. 1 shows the current waveforms of WT-1, WT-2, WT-3, and WT-4 along with their FFT analysis before t = 4 s. As the PFs of the WTs in the frequency-domain are not the same, the THDs of the currents are also not the same. The WT-4 current and the WT-3 current have the largest and the smallest THD in the time-domain, respectively, which is also predicting by the proposed PF analysis in Table 3. 1. In Figure 3. 1, at t = 4 s, WT-1, i.e., the WT with the smallest PF, is disconnected from the WPP. As it can be seen, in this case, the electrical oscillations in the WPP are not eliminated and are remained in the system.

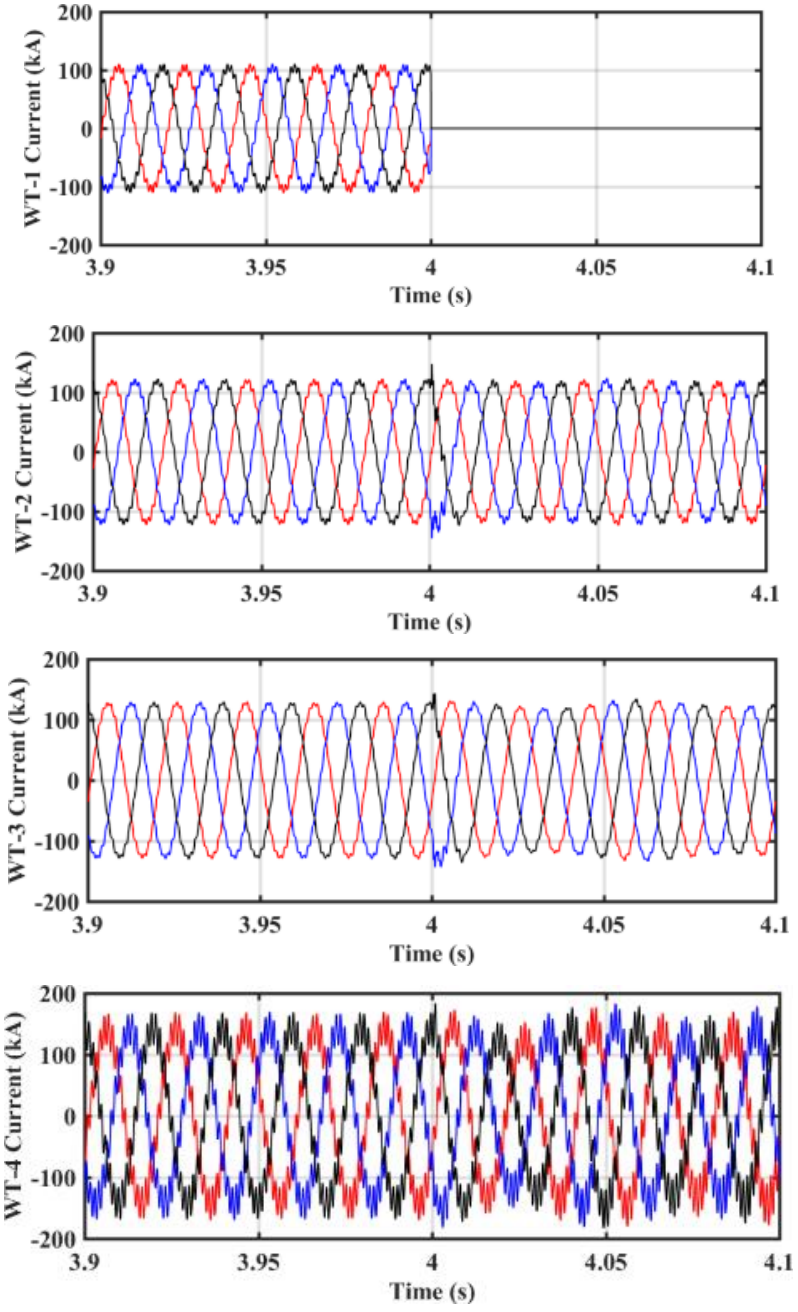
WT-1 Current (kA)
WT-2 Current (kA)
WT-3 Current (kA)
WT-4 Current (kA)
200
100
0
-100
-200
3.9
3.95
4
4.05
4.1
Time (s)

(a)

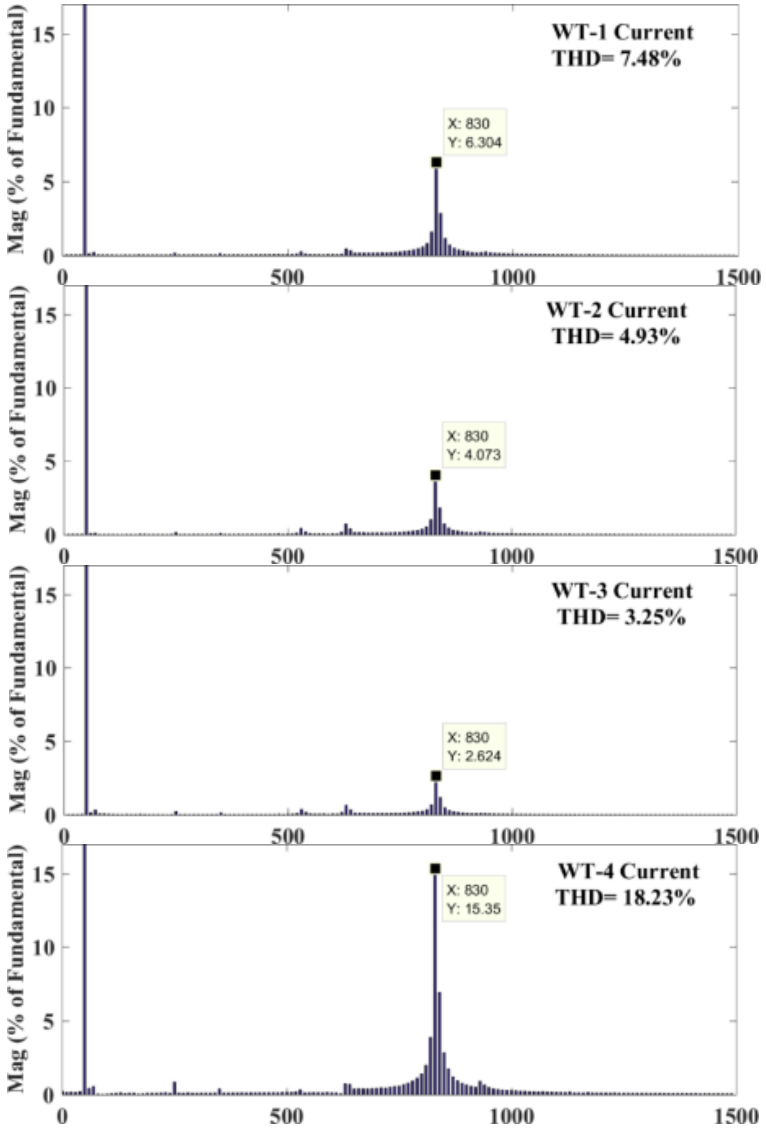

(b)

Figure 3. 1: The current waveforms of WT-1, WT-2, WT-3, and WT-4, and their FFT analysis, (a) the current waveforms, where WT-1 is disconnected at t = 4 s, (b) FFT analysis of the current waveforms before t = 4 s [98].

However, in Figure 3. 2, WT-4, i.e., the WT with the largest PF, is disconnected from the WPP. Figure 3. 2 shows that the electrical oscillations will be mitigated and damped in the WPP, which confirms that WT-4 is the main source of oscillations, as predicted in Table 3. 1.

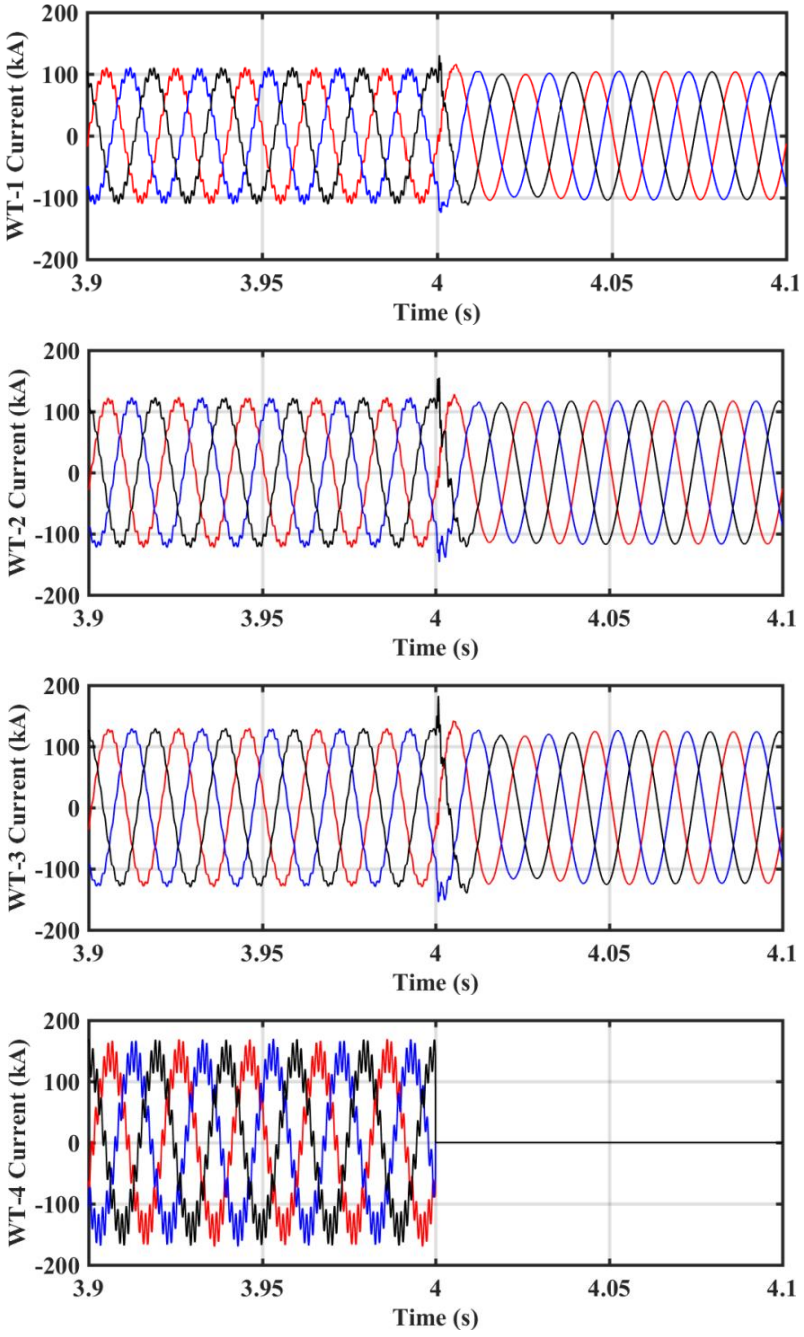

Figure 3. 2: The currents waveforms of WT-1, WT-2, WT-3, and WT-4, where WT-4 is disconnected at t = 4 s [98].

3.4. RESONANCE MODE ANALYSIS

3.4.1. PAPER 4

Title: Dynamic resonance sensitivity analysis in wind farms

E. Ebrahimzadeh, F. Blaabjerg, X. Wang, and C. L. Bak
in Proc. of IEEE PEDG Conference, Brazil, 2017, pp. 1-6.

✓ Contributions

- Performing the sensitivity analysis to identify which bus excites the resonances more
- Identifying the best candidate bus to do the passive or active passive damping to reduce the resonance problems

✓ Results

In this part, the electrical resonances of the WPP are identified by the proposed resonance analysis. Figure 3. 3 shows that the WPP has the resonance frequencies at f = 945 Hz, f = 1425 Hz, f = 1705 Hz, and f = 1985 Hz.

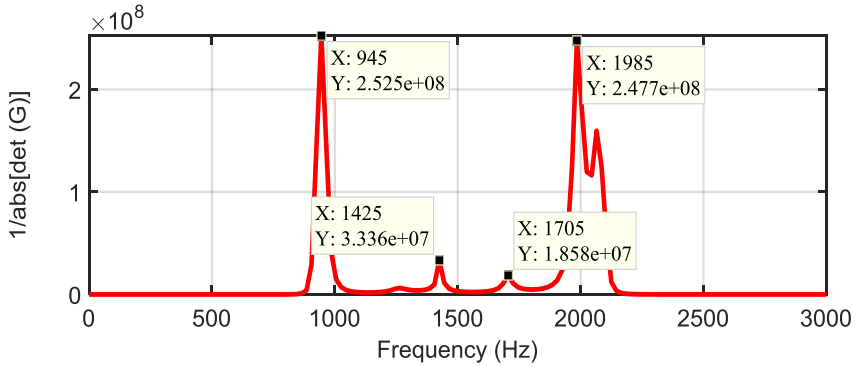

Figure 3. 3: Resonance analysis of the 400-MW WPP by the proposed method [110].

In order to identify which buses excite the resonances more, the PF analysis has been carried out and the results are shown in Table 3. 2. In this case, as all parameters of the WTs are designed as the same, the structure of the WPP is symmetrical. Therefore, the buses 2 to 5, the buses 6 to 9 , and the buses 14 and 15 have the same PF values for different resonances. Table 3. 2 shows that the buses 10 to 13 have the largest PF for the resonance at f = 1705 Hz, the buses 2 to 5 have the smallest PF for the resonance at f = 1705 Hz. For the resonance at f = 1425 Hz, the bus 1 has a much

larger PF (PF= 0.945) than the other buses, which confirms that this bus amplifies considerably the disturbances around f = 1425 Hz.

Table 3. 2: Participation Factors (PFs) of the WPP buses for the electrical resonances, which have been identified in Figure 3. 3.

Resonance Frequency	PFs of Bus 2, 3, 4, 5	PFs of Bus 6, 7, 8, 9	PFs of Bus10, 11, 12, 13	PFs of Bus 14, 15	PF of Bus 16	PF of Bus 1	The most exciting bus	The least exciting bus
945 Hz	0.17665	0.125048	0.108174	0.021506	0	0	Bus 2, 3, 4, 5	Bus 1, 16
1425 Hz	0.002617	0.016014	0.02115	0.027876	0.00344	0.945	Bus 1	Bus 2, 3, 4, 5
1705 Hz	0.00433	0.103501	0.116046	0.036447	0.0565	0.0106	Bus10,11,12, 13	Bus 2, 3, 4, 5
1985 Hz	0.002168	0.111667	0.107783	0	0	0	Bus 6, 7, 8, 9	Bus 1, 14, 15, 16

In order to validate these frequency-domain analysis, the WPP is simulated in the PSCAD software and the results are shown in Figure 3. 4. In this scenario, the main gird voltage has 3% disturbance at f = 1705 Hz. The voltage waveforms of the buses 10, 6, 1, and 2, and their FFT are shown in Figure 3. 4. The voltage of bus 10 has the largest THD and the voltage of the bus 2 has the smallest THD, as expected from Table 3. 2.

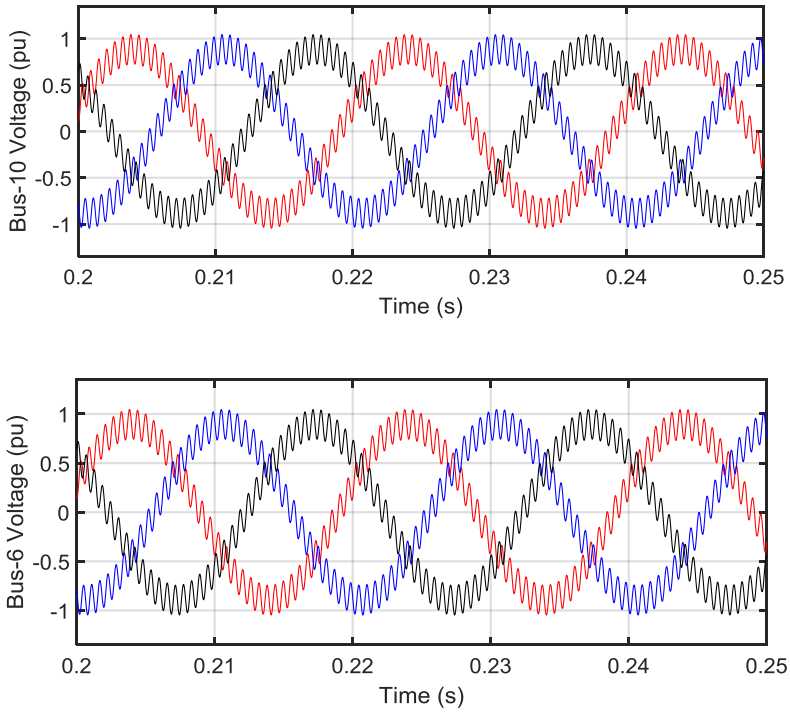

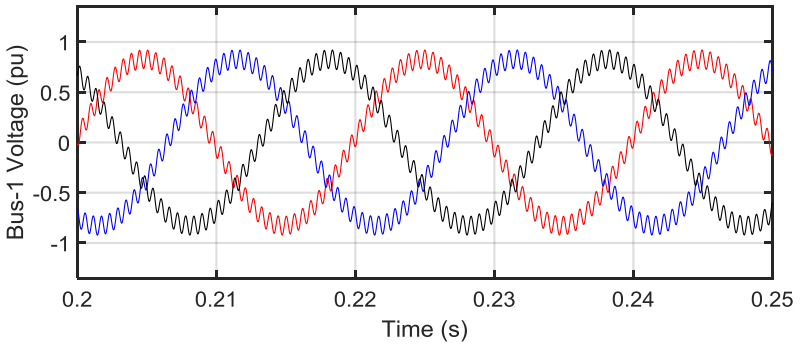
Bus-1 Voltage (pu)
1
0.5
0
-0.5
-1
0.2
0.21
0.22
0.23
0.24
0.25
Time (s)

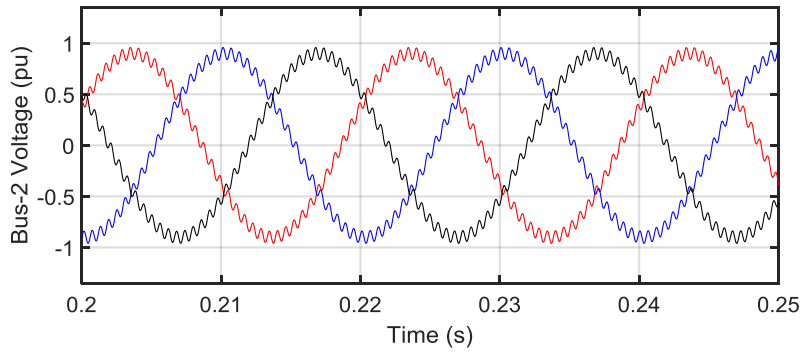
Bus-2 Voltage (pu)
1
0.5
0
-0.5
-1
0.2
0.21
0.22
0.23
0.24
0.25
Time (s)

(a)

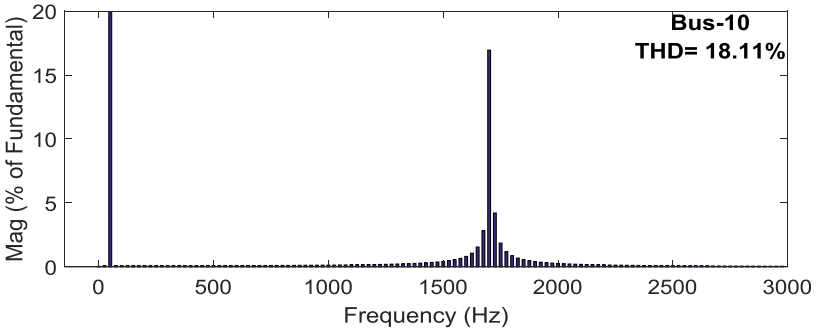
Bus-10
THD= 18.11%
Mag (% of Fundamental)
20
15
10
5
0
0
500
1000
1500
2000
2500
3000
Frequency (Hz)

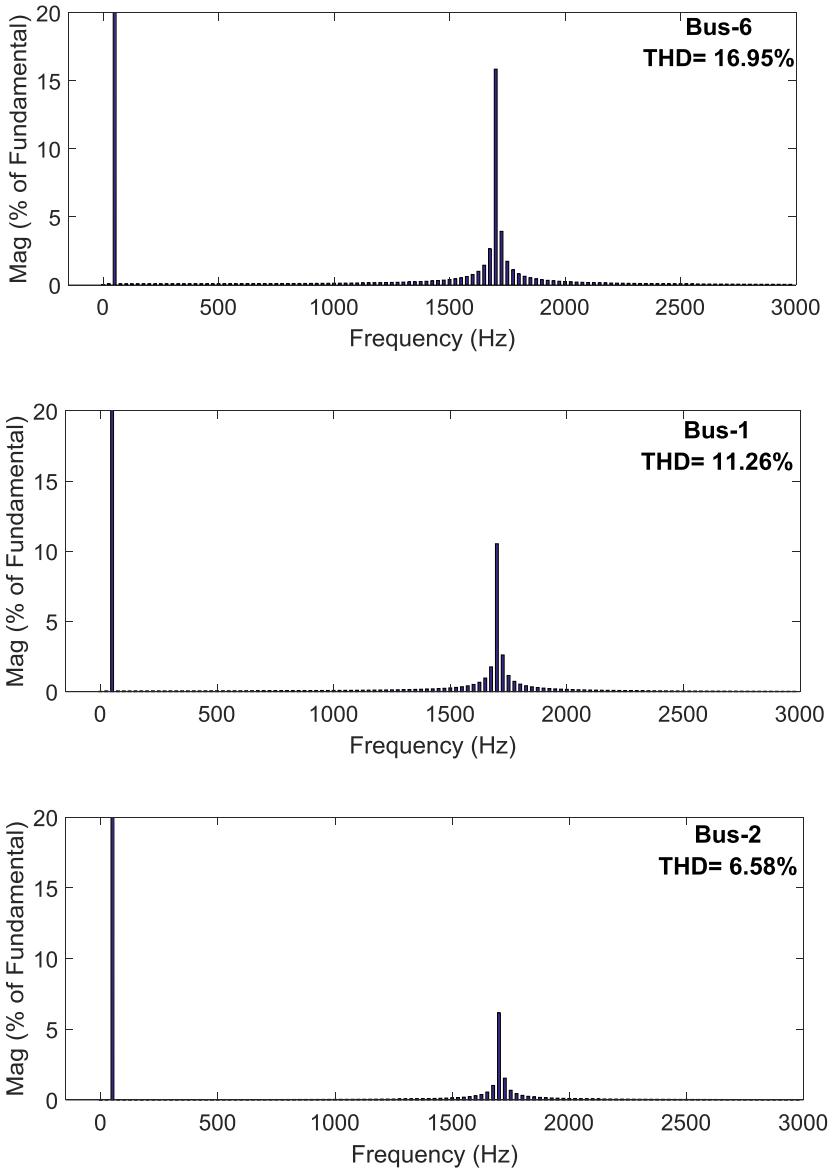

(b)

Figure 3. 4: The voltage waveforms for the buses 10, 6, 1, and 2 and their FFT analysis, where the grid voltage has 3% harmonics at f = 1705 Hz, (a) the voltage waveforms, (b) FFT analysis of the voltage waveforms [110].

CHAPTER 4. OPTIMIZATION AND MITIGATION

4.1. ABSTRACT

In order to damp and mitigate the oscillations and resonances, this chapter discusses an optimization procedure to redesign the controller parameters of WTs. The optimization is done in the frequency domain, where the objective is to put the oscillatory modes of the WPP in the suitable locations with acceptable damping. The proposed design enhances the stability margin and improves the dynamic response of the WPP. Time-domain simulations in the PSCAD software confirm the effectiveness of the presented algorithm.

4.2. PROPOSED METHOD FOR DESIGN

As it already discussed, the frequency (f_i) and the damping (ζ_i) of the oscillatory modes can be identified by

$$f_i = \frac{\beta_i}{2\pi} \qquad \zeta_i = \frac{-\alpha_i}{\sqrt{\alpha_i^2 + \beta_i^2}} \tag{4.1}$$

If the mode with the largest real part, P_c, has a negative real part, the system is stable as the real part of all other poles are smaller and more negative.

$$p_c = \alpha_c + j\beta_c \;\; \alpha_c = Max(\alpha_1, \alpha_2, \cdots, \alpha_q) \tag{4.2}$$

Therefore, in order to stabilize the WPP, the constraint H(x) in the optimization procedure is defined in (10) to make sure that all real parts are negative. In order to have a margin, it has been tried that the real parts are smaller than -10.

$$\alpha_c + 10 = H(x) \le 0 \tag{4.3}$$

The vector **x** is a vector of the optimization variables including the parameters of the power converters:

$$\mathbf{x} = [K_{p-k},\ K_{i-k},\ L_{f-k},\ C_{f-k}] \tag{4.4}$$

The dynamic response of a second-order system with different damping ratios has

been shown in Figure 4. 1. As it can be seen, a system with the smaller damping reaches to its final value faster but oscillates a lot around this value. A system with a larger damping reaches to the final value slower and smoother. Figure 4. 1 shows that the best trade-off between the speed and oscillations happens for damping around 0.8.

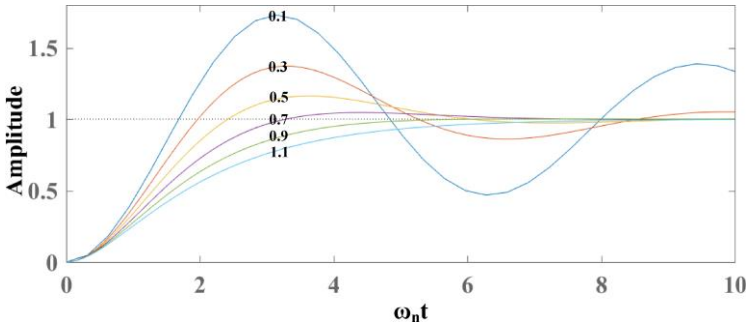

Figure 4. 1: Dynamic response of a second-order system for different dampings.

In a WPP, low-frequency and high-frequency oscillations correspond to the grid-connected converters and passive components, respectively [110]- [113]. Therefore, in order to guarantee the dynamic response of WTs in the WPP, an objective function is defined to set all low-frequency modes with damping around 0.8. The objective function is actually to minimize F(x), which defined as

$$F(x) = Max\left[\left|\zeta_1 - 0.8\right|, \left|\zeta_2 - 0.8\right|, \cdots, \left|\zeta_n - 0.8\right|\right]$$
$$\xi_j = \frac{-\alpha_j}{\sqrt{\alpha_j^2 + \beta_j^2}}, \quad f_j = \frac{\beta_j}{2\pi} < f_{h1} \cong 500Hz, \; j = 1, 2, ..., n \tag{4.5}$$

In the following sections, more details of the optimum design procedure are discussed in order to mitigate the oscillations and to reduce the resonances.

4.3. OSCILLATIONS MITIGATION

4.3.1. PAPER 5

Title: Optimum design of power converter current controllers in power electronics based power systems

E. Ebrahimzadeh, F. Blaabjerg, X. Wang, and C. L. Bak, submitted to IEEE Transactions on Industry Applications.

✓ Contributions

- Showing that a good design of the WTs under strong grid conditions cannot guarantee stable operation of whole WPP
- Damping the oscillations by a multi-objective optimization procedure to redesign the parameters of the WT controllers

✓ Results

Figure 4. 2 shows the mode damping ratios of the individual WT and the WPP for the stand-alone design (initial design). The damping ratios of the modes of the WPP for the optimized parameters (K_p = 9.51e-3, K_i = 4.16, and f_{res} = 357 Hz) are also shown in Figure 4. 2. As it can be seen, the damping ratios of the individual WT for the stand-alone design is around 0.8, which confirms that the individual WT for a strong grid has a good stability margin and an acceptable dynamic response. However, when all WTs are connected to the WPP, the damping ratios for low-frequency modes are too small and the damping ratio for the frequency around 900 Hz is negative, which shows that the WPP is unstable around this frequency. Therefore, it is necessary to redesign the controller parameters to improve the stability margin and to guarantee a desired dynamic response. As shown in Figure 4. 2, after setting the GSC parameters based on the proposed optimum design procedure, all modes have positive damping, which confirms that the WPP has a stable operation. In addition, the low-frequency modes, which is related to the power converter dynamics, have suitable dampings around 0.8, which depicts that the WPP has a desired dynamic performance for the optimum design.

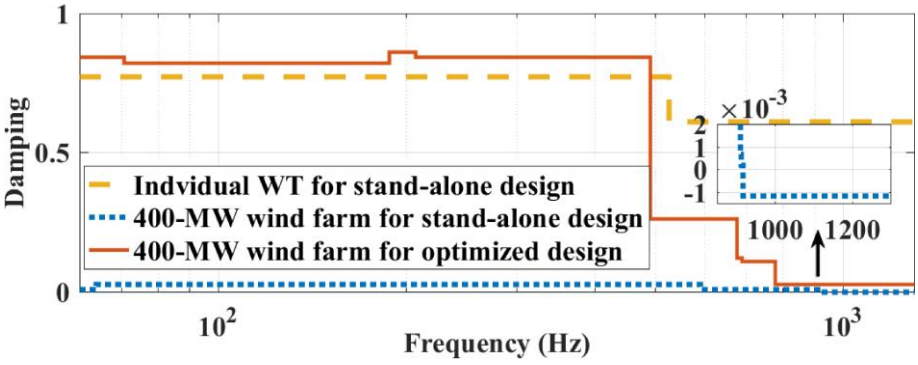

Figure 4. 2: Mode damping ratios of the individual WT and the WPP for the stand-alone design, and for the optimum design.

In Figure 4. 3, the WPP is simulated in the time-domain using PSCAD software, where the current controller parameters of the GSCs have been set by the proposed optimum design (before t = 0.5 s). At t = 0.4 s, the current reference is changed from 0.25 p.u. to 1 p.u. As it can be seen, the WPP has a good dynamic response and a stable operation for the optimized parameters. At t = 0.5, the GSC parameters are changed from the optimum design to the initial design. As shown in Figure 4.3, some

oscillations around 900 Hz propagate into the WPP, because of the instability problems as predicted in Figure 4. 2 in the frequency-domain.

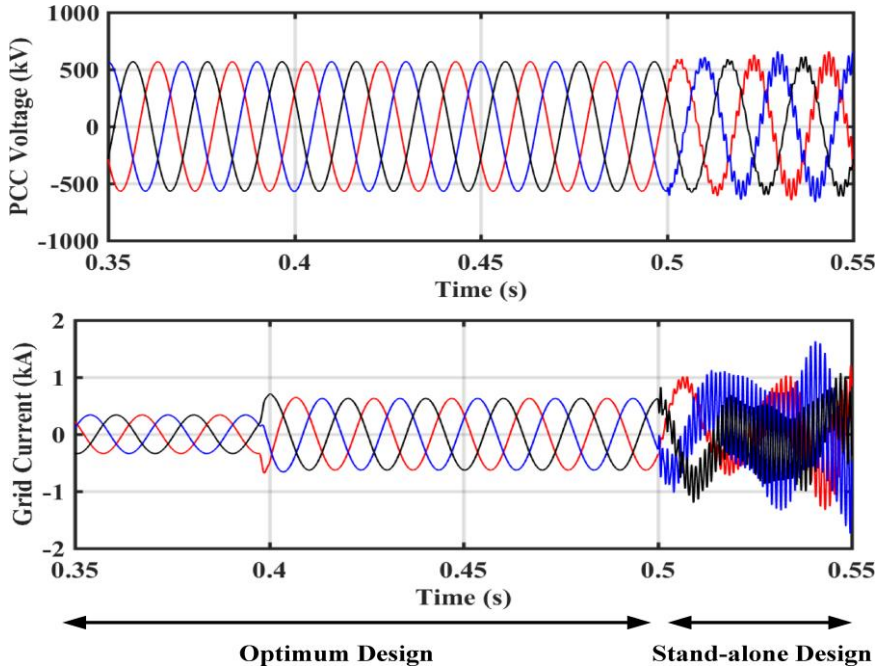

Figure 4. 3: Testing the dynamic response of the GSCs; the GSCs parameters are changed from the optimum design to the initial design at t = 0.5 s and the dynamic response of the optimum design is also tested at t = 0.4 s.

4.4. ROBUSTNESS OF THE OPTIMUM DESIGN

4.4.1. PAPER 6

Title: Reducing harmonic instability and resonance problems in PMSG based wind farms

E. Ebrahimzadeh, F. Blaabjerg, X. Wang, and C. L. Bak,
Journal of Emerging and Selected Topics in Power Electronics, vol. 6, no. 1, pp. 73-83, Mar. 2018.

✓ **Contributions**

- Minimizing the number of the resonances by a Genetic Algorithm (GA)

based optimization procedure

- Robustness analysis of the optimum design method against the WPP variations

✓ Results

In this section, the robustness of the optimum design case against variations of the WPP is studied. In order to confirm the robustness of the optimized design, the time-domain simulations have been performed. First, the GSC parameters are optimized and set for SCR = 5. However, at t = 1 s, SCR = 5 is changed to SCR = 4. As it can be seen from Figure 4. 4, the WPP with the optimum controller design presents a robust and stable operation for such variations.

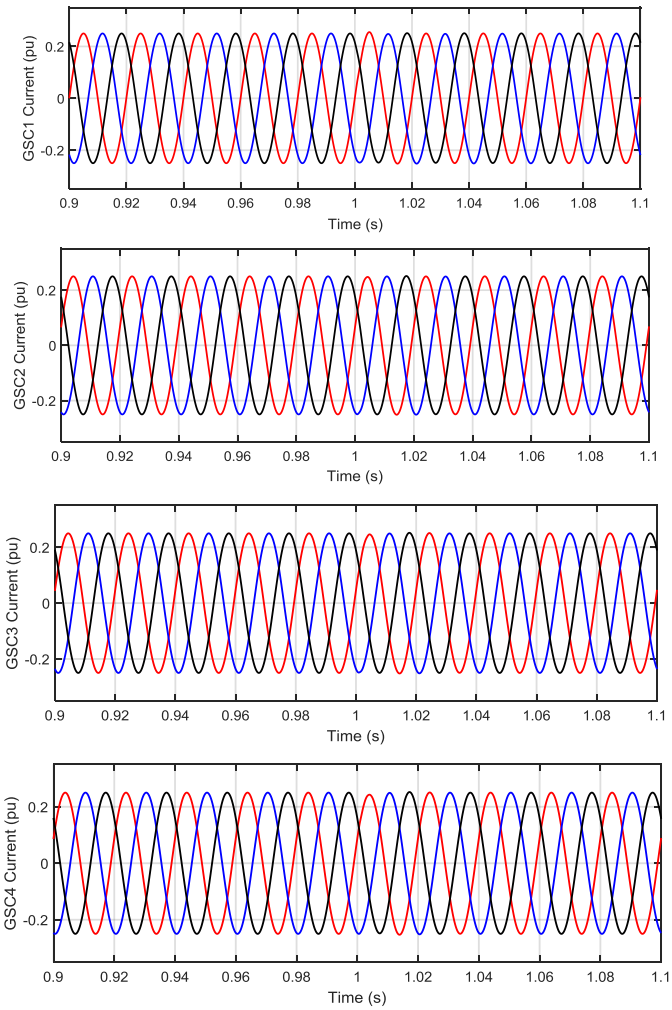

Figure 4. 4: Robustness of the optimum design. The GSC parameters are optimized and set for SCR = 5 but the SCR is changed from 5 to 4 at t = 1 s [112].

CHAPTER 5. CONCLUSION

5.1. SUMMARY

As the number of WTs and WPPs are increasing in the power grid, power quality issues are becoming more and more important. Among power quality issues, electrical oscillations are common phenomena in WPPs. This thesis models, controls, and mitigates the electrical oscillations around and above the fundamental frequency.

In Chapter 1, the background, motivation, objective, and the limitation of the project is described. Also, the case study of the project, which is a 400-MW WPP, is presented.

In Chapter 2, a general and simple method in the frequency-domain is presented to model and analyze electrical oscillations in WPPs. Several case studies are considered to find the effects of different variations on electrical oscillations. The analysis and simulation results show that increasing the number of WTs, cable lengths and controller bandwidths, as well as, decreasing the grid SCR can amplify the oscillations and resonances in the WPP.

In Chapter 3, Participation factor (PF) analysis and sensitivity analysis are presented to identify which bus or which WT in a WPP has more contribution to the electrical oscillations or which bus can excite the resonances more. PF analysis and simulation results show that disconnecting a WT with the largest PF can damp the oscillations. In addition, the results confirm that a bus with a larger PF has higher impact on the resonances.

In Chapter 4, an optimum design procedure in the frequency-domain has been presented to reduce electrical oscillations and enhance the stability margin. The results show that the optimum design can guarantee the stability and the desired dynamic response of the WPP, as well as the optimum design is robust against variations of the system.

5.2. THESIS CONTRIBUTIONS

The main contributions of this thesis can be highlighted as follows:

- In spite of the previous works, where stability analysis of the power system is discussed based on the state-space modelling, this thesis introduces the WPP as a Multi-Input Multi-Output (MIMO) transfer function matrix. The oscillatory modes of the WPP are identified by the determinant of the MIMO matrix and the resonances are identified by the element amplitudes of the MIMO matrix.

- As the proposed modelling method is based on the nodal admittance matrix of the system, a large WPP can easily be modeled. When a component of the WPP is changed, just one element of the MIMO transfer function matrix is affected. Therefore, the analysis of WPPs under different conditions can be easily performed. When a component of the WPP is a black-box, its equivalent admittance (transfer function) can be obtained by experiment or by time-domain simulations.

- Most literatures about the stability of WPPs have been paid less attention to the time-delay of the PWM and the discrete control system. However, in a few papers about the individual power electronic converters, it has been demonstrated that the time-delay has a significant effect on the stability of the converter. In order to fill in this gap, in this thesis, a frequency-domain modelling method for large WPPs is presented, which also considers the delay of the PWM and the delay of the discrete implementation. The effects of the number of the WTs, SCR variations, cable lengths, PLL, and controller bandwidths are also discussed.

- Participation Factor (PF) and sensitivity analysis of different buses can be used to locate the main source of the electrical oscillations and to find the most suitable location to install active or passive filters in the power system. The proposed PF analysis can predict the transient oscillations during faults and voltage sags. The amplification of the grid background distortion by the electrical resonances are analyzed by the sensitivity analysis to identify the most excited bus.

- A multi-objective optimization methodology is proposed to redesign the power converter parameters to guarantee the stable operation of WPP, to reduce the electrical oscillations, and to improve the dynamic response. As the presented frequency-domain based optimum design method is simple and has low computational burden, it is possible to apply this method to large WPPs. In addition, the optimum controller design is robust against the variations of the WPP.

5.3. FUTURE WORKS

Some possible future works related to the oscillations are listed as follows:

- This work has discussed electrical oscillations around the fundamental frequency and above. However, as wind variations and generator shaft in a WPP can lead to very low frequency oscillations, it is worth to analyze such oscillations as well.

- This work discusses a WPP, where all power converters are voltage-source converters. A new research can be defined to study a general power electronics based power system, where both voltage-source converters and current-source converters are included.

- In very large WPPs, the order of the proposed modeling would be large. Therefore, it would be an interesting work on reducing the order of the model and keep the accuracy at the same time.

- As the electrical grid is assumed to be balanced in this project, a new study can be defined to analyze the effects of the unbalanced grid and also fault conditions.

- In this project, a PMSG based wind power plant connected to the electrical grid is considered as a case study. Therefore, the analysis of HVDC connected wind power plants, DFIG based wind power plants, or stand-alone wind power plants can also be studied as new research topics and then the proposed method in this thesis can be applied.

- In this thesis, the Synchronous Reference Frame Phase-Locked Loop (SRF-PLL) is modeled and its effect is discussed. However, modeling and analysis of power converters with different grid synchronization methods would be an interesting research topic too, as they might effect on the overall stability of the WPP.

- Frequency-domain modeling of saturations and nonlinear dynamics, PWM, dc-link oscillations, and the dead-time in the IGBT modules can be useful to investigate in order to model the overall behavior of the wind turbines more accurate.

- In this thesis, every string of the 400-MW WPP was aggregated as one 100-MW wind turbine, where was assumed that all WTs on each string generate the nominal power. The used aggregation model can identify the overall behavior of the string of the WPP but some internal interaction dynamic modes may be eliminated. Therefore, it would be an interesting topic to compare the dynamic response of the detailed and aggregated models of the string of the WPP, especially when the WTs generate different power values.

- In order to assess the proposed methods, which were discussed in this thesis, under more realistic conditions, Real Time Digital Simulator (RTDS) platform can be used or experimental measurements for a simplified system can be carried out.

BIBLIOGRAPHY

[1] B. K. Bose, “Global energy scenario and impact of power electronics in 21st century,” *IEEE Trans. Ind. Electron*., vol. 60, no. 7, pp. 2638–2651, Jul. 2013.

[2] J. M. Carrasco, L. G. Franquelo, J. T. Bialasiewicz, E. Galvan, R. C. Portillo Guisado, M. A. M. Prats, J. I. Leon, and N. Moreno-Alfonso, “Power-electronic systems for the grid integration of renewable energy sources: A survey,” *IEEE Trans. Ind. Electron*., vol. 53, no. 4, pp. 1002– 1016, Jun. 2006.

[3] R. H. Renner and D. Van Hertem, "Ancillary services in electric power systems with HVDC grids," *IET Gen. Transm. Distrib.*, vol. 9, no. 11, pp. 1179-1185, Aug. 2015.

[4] E. Ebrahimzadeh, S. Farhangi, H. Iman-eini, F. B. Ajaei, and R. Iravani, “Improved phasor estimation method for dynamic voltage restorer applications,” *IEEE Trans. Power Deliv.*, vol. 30, no. 3, pp. 1467–1477, Oct. 2015.

[5] M.S. Mahmoud, S. Azher Hussain, and M.A. Abido, “Modeling and control of microgrid: An overview,” *J. Franklin. Inst*., vol. 351, no. 5, pp. 2822-2859, May. 2014.

[6] D. Ronanki, S. A. Singh, and S. S. Williamson, "Comprehensive topological overview of rolling stock architectures and recent trends in electric railway traction systems," *IEEE Trans. Transport. Electrific*, vol. 3, no. 3, pp. 724-738, Sep. 2017.

[7] I. Boldea, "Electric generators and motors: An overview," *CES Trans. Electr. Machin. and Syst*., vol. 1, no. 1, pp. 3-14, Mar. 2017.

[8] http://gwec.net/

[9] J. Mohammadi, S. Afsharnia, E. Ebrahimzadeh, and F. Blaabjerg, “An enhanced LVRT scheme for DFIG-based WECSs under both balanced and unbalanced grid voltage sags,” *Electr. Powe. Comp. Syst*, vol. 45, no. 11, pp. 1242-1252, Jul. 2017.

[10] E. Z. Bighash, S. M. Sadeghzadeh, E. Ebrahimzadeh, and F. Blaabjerg, “A novel predictive control for single phase grid-connected photovoltaic inverters,” *in Proc. of IEEE ECCE Conference*, USA, 2017, pp. 1-7.

[11] E. Z. Bighash, S. M. Sadeghzadeh, E. Ebrahimzadeh, and F. Blaabjerg, “LVRT capability of single-phase grid-connected HERIC inverter in PV systems by a look-up table based predictive control,” i*n Proc. of IEEE IECON Conference*, China, 2017, pp. 1-6.

[12] F. Blaabjerg, R. Teodorescu, M. Liserre, and A. V. Timbus, “Overview of control and grid synchronization for distributed power generation systems,” *IEEE Trans. Ind. Electron*., vol. 53, no. 5, pp. 1398–1409, Oct. 2006.

[13] T. Messo, J. Jokipii, J. Puukko, and T. Suntio, “Determining the value of dc-link capacitance to ensure stable operation of a three-phase photovoltaic inverter, *IEEE Trans. Power Electron*., vol. 29, no. 2, pp. 665–673, Feb. 2014.

[14] D. Bazargan, S. Filizadeh, and A. M. Gole, “Stability analysis of converter-connected battery energy storage systems in the grid,” *IEEE Trans. Sustain. Energy*, vol. 5, no. 4, pp. 1204–1212, Oct. 2014.

[15] P. Kundur, Power system stability and control, 1994, McGrawHill.

[16] E. Ebrahimzadeh and F. Blaabjerg, "Reactive power role and its controllability in AC power transmission systems ", *Reactive Power Control in AC Power Systems*, Springer, 2017, pp. 117-136.

[17] D. Biggar and M. Hesamzadeh, Introduction to electric power systems, 2014, Wiley-IEEE Press.

[18] Z. Chen, F. Blaabjerg, and Y. Hu, “Stability improvement of wind turbine systems by STATCOM,” *in Proc. of IEEE IECON Conference*, 2006, pp. 4213–4218.

[19] F. A. L. Jowder, “Influence of mode of operation of the SSSC on the small disturbance and transient stability of a radial power system,” *IEEE Trans. Power Syst.*, vol. 20, no. 2, pp. 935–942, 2005.

[20] H. Novanda, P. Regulski, V. Stanojevic, and V. Terzija, "Assessment of frequency and harmonic distortions during wind farm rejection test," *IEEE Trans. Sustain. Energy*, vol. 4, no. 3, pp. 698-705, Jul. 2013.

[21] G. Quinonez-Varela, G. Ault, O. Anaya-Lara, and J. McDonald, "Electrical collector system options for large offshore wind farms," *IET Renew. Power Gener*., vol. 1, no. 2, pp. 107–114, Jun. 2007.

[22] S. Kuenzel, L. P. Kunjumuhammed, B. C. Pal, and I. Erlich, "Impact of wakes on wind farm inertial response," *IEEE Trans. Sustain. Energy*, vol. 5, no. 1, pp. 237–245, Jan. 2014

[23] S. Hao, Y. Zhang, X. Li, and Y. Yuan, "Equivalent wind speed model in wind farm dynamic analysis," *in Proc. of IEEE DRPT*, 2011, pp. 1751– 1755.

[24] J. K. Sethi, D. Deb, and M. Malakar, "Modeling of a wind turbine farm in presence of wake interactions," *in Proc. of ICEAS Conference*, 2011, pp. 1–6.

[25] E. Muljadi, C. P. Butterfield, A. Ellis, J. Mechenbier, J. Hochheimer, R. Young, N. Miller, R. Delmerico, R. Zavadil, and J. C. Smith "Equivalencing the collector system of a large wind power plant," *in Proc. of IEEE PES GM Conference*, 2006, p. 9.

[26] F. Mei and B. Pal, "Modal analysis of grid-connected doubly fed induction generators," *IEEE Trans. Energy Convers*., vol. 22, no. 3, pp. 728–736, Sep. 2007.

[27] V. Akhmatov and H. Knudsen, "An aggregate model of a grid-connected, large-scale, offshore wind farm for power stability investigations: Importance of windmill mechanical system," *Int. J. Elect. Power Energy Syst*., vol. 24, no. 9, pp. 709–717, Nov. 2002.

[28] J. H. R. Enslin and P. J. M. Heskes, "Harmonic interaction between a large number of distributed power inverters and the distribution network," *IEEE Trans. Power Electron.*, vol. 19, no. 6, pp. 1586–1593, Nov. 2004.

[29] HOPEWIND, "Several key technical problems of grid-connected inverter," *China wind Power Center*. [Online]. Available: http://www.cwpc.cn/cwpp/files/1314/1050/5552/6.-.pdf.

[30] C. F. Jensen, Ł. H. Kocewiak, and Z. Emin, "Amplification of harmonic background distortion in wind power plants with long high voltage connections," *CIGRE Biennial Session, CIGRÉ*, 21-26 August 2016, Paris, France, C4-112.

[31] T. Tsanova, "Germany's DolWin2 offshore link is off for repairs," 2016. [Online].Available:http://renewables.seenews.com/news/germanysdolwin2-offshore-link-is-off-for-repairs-529905.

[32] I. Shumkov, "Dong's Anholt offshore wind farm shuts down due to new cable fault," 2015. [Online]. Available: http://renewables.seenews.com/news/dongs-anholt-offshore-wind-farmshuts-down-due-to-new-cable-fault-464750.

[33] M. Larsson, 'Harmonic resonance and control interoperability analysis for HVDC connected wind farms' *IEEE Workshop eT&D*, 7-9 November, 2017, Aalborg, Denmark.

[34] L. H. Kocewiak, J. Hjerrild, and C. L. Bak, "Wind turbine converter control interaction with complex wind farm systems," *IET Renew. Power Gener*., vol. 7, no. 4, pp. 380–389, Jul. 2013.

[35] R. C. Dugan, M. F. McGranaghan, S. Santoso, and H. W. Beaty, *Electrical Power Systems Quality, Second Edition*, Mc Graw-Hill.

[36] P. Li, Y. D. Song, D. Y. Li, W. C. Cai, and K. Zhang, "Control and monitoring for grid-friendly wind turbines: research overview and suggested approach," *IEEE Trans. Power Electron.*, vol. 30, no. 4, pp. 1979-1986, Apr. 2015.

[37] S. B. Naderi, M. Negnevitsky, A. Jalilian, M. Tarafdar Hagh, and K. M. Muttaqi, "Optimum resistive type fault current limiter: An efficient solution to achieve maximum fault ride-through capability of fixed-speed wind turbines during symmetrical and asymmetrical grid faults," *IEEE Trans. Ind. Appl.*,, vol. 53, no. 1, pp. 538-548, Jan.-Feb. 2017.

[38] Z. Chen, M. Yin, Y. Zou, K. Meng, and Z. Dong, "Maximum wind energy extraction for variable speed wind turbines with slow dynamic behavior," *IEEE Trans. Power Syst.*, vol. 32, no. 4, pp. 3321-3322, Jul. 2017.

[39] Y. Song, E. Ebrahimzadeh, and F. Blaabjerg, “Analysis of high frequency resonance in DFIG-based offshore wind farm via long transmission cable,” *IEEE Trans. Energy Convers*., 2018, early access.

[40] S. Mondal and D. Kastha, "Maximum active and reactive power capability of a matrix converter-fed DFIG-based wind energy conversion system," *IEEE J. Emerg. Sel. Topics Power Electron.*, vol. 5, no. 3, pp. 1322-1333, Sep. 2017.

[41] H. A. Mohammadpour and E. Santi, "SSR damping controller design and optimal placement in rotor-side and grid-side converters of series-compensated DFIG-based wind farm," *IEEE Trans. Sustain. Energy*, vol. 6, no. 2, pp. 388-399, Apr. 2015.

[42] Z. Zhang, F. Wang, J. Wang, J. Rodríguez, and R. Kennel, "Nonlinear direct control for three-level NPC back-to-back converter PMSG wind turbine systems: experimental assessment with FPGA," *IEEE Trans. Ind. Informat.*, vol. 13, no. 3, pp. 1172-1183, Jun. 2017.

[43] M. Davari and Y. A. R. I. Mohamed, "Robust DC-link voltage control of a full-scale PMSG wind turbine for effective integration in DC grids," *IEEE Trans. Power Electron*., vol. 32, no. 5, pp. 4021-4035, May 2017.

[44] G. C. Konstantopoulos and A. T. Alexandridis, "Full-scale modeling, control, and analysis of grid-connected wind turbine induction generators with back-to-back AC/DC/AC converters," *IEEE Trans. Emerg. Sel. Topics Power Electron.*, vol. 2, no. 4, pp. 739-748, Dec. 2014.

[45] P. Xing, L. Fu, G. Wang, Y. Wang, and Y. Zhang, "A compositive control method of low-voltage ride through for PMSG-based wind turbine generator system," *IET Gen. Transm. Distrib.*,vol. 12, no. 1, pp. 117-125, Feb. 2018.

[46] L. Yu, R. Li and L. Xu, "Distributed PLL-based control of offshore wind turbine connected with diode-rectifier based HVDC systems," *IEEE Trans. Power Del.*, 2018, early access.

[47] J. Wang, J. D. Yan, L. Jiang, and J. Zou, “Delay-dependent stability of single-loop controlled grid-connected inverters with LCL filters,” *IEEE Trans. Power Electron.*, vol. 31, no. 1, pp. 743–757, Jan. 2016.

[48] R. Bhushan and K. Chatterjee, "Effects of parameter variation in DFIG-based grid connected system with a FACTS device for small-signal stability analysis," *IET Gen. Transm. Distrib.*, vol. 11, no. 11, pp. 2762-2777, Mar. 2017.

[49] Y. Song and F. Blaabjerg, "Overview of DFIG-based wind power system resonances under weak networks," *IEEE Trans. Power Electron*., vol. 32, no. 6, pp. 4370-4394, Jun. 2017.

[50] J. Follum, J. W. Pierre and R. Martin, "Simultaneous estimation of electromechanical modes and forced oscillations," *IEEE Trans. Power Syst.*, vol. 32, no. 5, pp. 3958-3967, Sep. 2017.

[51] W. Du, X. Chen, and H. F. Wang, "Impact of dynamic interactions introduced by the DFIGs on power system electromechanical oscillation modes," *IEEE Trans. Power Syst.*, vol. 32, no. 6, pp. 4954-4967, Nov. 2017.

[52] X. Wang, F. Blaabjerg, and W. Wu, “Modelling and analysis of harmonic stability in ac power-electronics-based power system,” *IEEE Trans. Power Electron*., vol. 29, no. 12, pp.6421 -6432, Dec. 2014.

[53] L. Monjoa, L. Sainza, J. Liangb, and J. Pedraa, " Study of resonance in wind parks," *Elect. Power Syst. Res*., vol. 128, pp. 30–38, Nov. 2015.

[54] W. Xu, Z. Huang, Y. Cui, and H. Wang, "Harmonic resonance mode analysis," *IEEE Trans. Power Del*., vol. 20, no. 2, pp. 1182-1190, Apr. 2005.

[55] Y. Cui and X. Wang, “Modal frequency sensitivity for power system harmonic resonance analysis,” *IEEE Trans. Power Del.*, vol. 27, no. 2, pp. 1010–1017, Apr. 2012.

[56] S. A. Papathanassiou and M.P Papadopoulos, “Harmonic analysis in a power system with wind generation”, *IEEE Trans. Power Del.*,vol. 21, no. 4, 2006.

[57] K. N. B. M. Hasan, K. Rauma, A. Luna, J. I. Candela, and P. Rodriguez,“Harmonic compensation analysis in offshore wind power plants using hybrid filters,” *IEEE Trans. Ind. Appl.*, vol. 50, no. 3, pp. 2050–2060, May/Jun. 2014.

[58] X. Wu, X. Li, X. Yuan, and Y. Geng, "Grid harmonics suppression scheme for LCL-type grid-connected inverters based on output admittance revision," *IEEE Trans. Sustain. Energy*, vol. 6, no. 2, pp. 411-421, Apr. 2015.

[59] H. Jinwei, Y. W. Li, D. Bosnjak, and B. Harris, "Investigation and active damping of multiple resonances in a parallel-inverter-based microgrid," *IEEE Trans. Power Electron.*, vol. 28, no. 1, pp. 234–246, Jan. 2013.

[60] S. Zhang, S. Jiang, X. Lu, B. Ge, and F. Z. Peng, "Resonance issues and damping techniques for grid-connected inverters with long transmission cable," *IEEE Trans. Power Electron*., vol. 29, no. 1, pp. 110–120, Jan. 2014.

[61] L. Xu and L. Fan, "Impedance-based resonance analysis in a VSC-HVDC system," *IEEE Trans. Power Del*., vol. 28, no. 4, pp. 2209–2216, Oct. 2013.

[62] L. Xu, L. Fan and Z. Miao, "DC impedance-model-based resonance analysis of a VSC–HVDC system," *IEEE Trans. Power Del.*, vol. 30, no. 3, pp. 1221-1230, June 2015.

[63] E. Ebrahimzadeh, F. Blaabjerg, X. Wang, C. L. Bak, "Efficient approach for harmonic resonance identification of large wind power plants," *in Proc. IEEE PEDG Conference*, Canada, 2016, pp. 1-7.

[64] C. Yoon, H. Bai, R. Beres, X. Wang, C. L. Bak, and F. Blaabjerg, "Harmonic stability assessment for multi-paralleled, grid-connected inverters," *IEEE Trans. Sustain. Energy*, vol. 7, no. 4, pp. 1388-1397, Oct. 2016.

[65] M. Cespedes and J. Sun, "Impedance modeling and analysis of grid connected voltage-source converters," *IEEE Trans. Power Electron.*, vol. 29, no. 3, pp. 1254–1261, Mar. 2014.

[66] D. Bazargan, S. Filizadeh, and A. M. Gole, "Stability analysis of converter-connected battery energy storage systems in the grid," *IEEE Trans. Sustain. Energy*, vol. 5, no. 4, pp. 1204-1212, Oct. 2014.

[67] J. Sun, "Impedance-based stability criterion for grid-connected inverters," *IEEE Trans. Power Electron.*, vol. 26, no. 11, pp. 3075–3078, Nov. 2011.

[68] M. Corradini, P. Mattavelli, M. Corradin, and F. Polo, "Analysis of parallel operation of uninterruptible power supplies loaded through long wiring cables," *IEEE Trans. Power Electron.*, vol. 25, no. 4, pp. 1046–1054, Apr. 2010.

[69] E. Ebrahimzadeh, F. Blaabjerg, X. Wang and C. L. Bak, "Modeling and identification of harmonic instability problems in wind farms," *in Proc. of IEEE ECCE Conference*, Milwaukee, WI, USA, 2016, pp. 1-6.

[70] X. Wang. F. Blaabjerg, M. Liserre, Z. Chen, J. He, and Y. W. Li, "An active damper for stabilizing power-electronics-based AC systems," *IEEE Trans. Power Electron*., vol. 29, no. 7, pp. 3318-3329, Jul. 2014.

[71] B. Badrzadeh, M. Gupta, N. Singh, A. Petersson, L. Max, and M. Høgdahl, "Power system harmonic analysis in wind power plants — Part I: Study methodology and techniques," in *Proc. of IEEE IAS*, 2012, pp. 1-11.

[72] D. S. Smith, M. K. Jenkins, and D. Howe, "The transient time domain analysis of non-linear electro-mechanical systems," *IEEE Trans. Magn.*, vol. 30, no. 5, pp. 3260-3263, Sep. 1994.

[73] F. J. Ferreira Pereira, J. M. Rodrigues, K. L. Miranda de Oliveira, D. R. Ribeiro Penido Araujo, and L. R. de Araujo, "Simulations and analysis of distribution systems with aspects of smart grids using MICQ, RTDS and PSCAD," *in Proc. of IEEE ISGT Conference*, Brazil, 2013, pp. 1-8.

[74] Q. Zhang, G. Lu, and C. Zhang, "Simulated study of the multiple cascade medium-voltage inverter based on PSCAD/EMTDC," *in Proc. of IEEE ICEMS*, Japan, 2016, pp. 1-6.

[75] P. Mitra, L. Zhang, and L. Harnefors, "Offshore wind integration to a weak grid by VSC-HVDC links using power-synchronization control: a case study," *IEEE Trans. Power Del.*, vol. 29, no. 1, pp. 453-461, Feb. 2014.

[76] X. Zhao, Z. Yan, Y. Xue, and X. P. Zhang, "Wind power smoothing by controlling the inertial energy of turbines with optimized energy yield," *IEEE Access*, vol. 5, pp. 23374-23382, 2017.

[77] P. Wang, X. P. Zhang, P. F. Coventry, and R. Zhang, "Start-up control of an offshore integrated MMC multi-terminal HVDC system with reduced DC voltage," *IEEE Trans. Power Syst.*, vol. 31, no. 4, pp. 2740-2751, Jul. 2016.

[78] P. Hou, E. Ebrahimzadeh, X. Wang, F. Blaabjerg, J. Fang, and Y. Wang, "Harmonic stability analysis of offshore wind farm with CCM," *in Proc. of IEEE IECON Conference, China, 2017*, pp. 1-6.

[79] N. Pogaku, M. Prodanovic, and T. C. Green, "Modeling, analysis and testing of autonomous operation of an inverter-based microgrid," *IEEE Trans. Power Electron.*, vol. 22, no. 2, pp. 613–625, Mar. 2007.

[80] N. Bottrell, M. Prodanovic, and T. C. Green, "Dynamic stability of a microgrid with an active load," *IEEE Trans. Power Electron*., vol. 28, no.11, pp. 5107-5119, Nov. 2013.

[81] A. Singh, and A. K. Kaviani, and B. Mirafzal, "On dynamic models and stability analysis of three-phase phasor PWM-based CSI for stand-alone applications," *IEEE Trans. Ind. Electron.*, vol. 62, no. 5, pp. 2698-2707, May. 2015.

[82] E. A. A. Coelho, P. C. Cortizo, and P. F. D. Garcia, "Small-signal stability for parallel-connected inverters in stand-alone AC supply systems," *IEEE Trans. Ind. App.*, vol. 38, no. 2, pp. 533-542, Mar. 2002.

[83] E. Ebrahimzadeh, F. Blaabjerg, X. Wang, and C. L. Bak, "Harmonic stability and resonance analysis in large PMSG-based wind power plants," *IEEE Trans. Sustain. Energy*, vol. 9, no. 1, pp. 12-23, Jan. 2018.

[84] E. Ebrahimzadeh, F. Blaabjerg, X. Wang, C. L. Bak, T. Lund, G. K. Andersen, C. G. Suárez, and J. Berg "Small signal modeling of wind farms," *in Proc. of IEEE ECCE Conference*, USA, 2017, pp. 1-7.

[85] L. P. Kunjumuhammed, B. C. Pal, C. Oates, and K. J. Dyke, "The adequacy of the present practice in dynamic aggregated modeling of wind farm systems," *IEEE Trans. Sustain. Energy*, vol. 8, no. 1, pp. 23-32, Jan. 2017.

[86] J. Kwon, X. Wang, F. Blaabjerg, C. L. Bak, A. R. Wood, and N. Watson, "Linearized modeling methods of ac-dc converters for an accurate frequency response," *IEEE J. Emerg. Sel. Topics Power Electron.*, vol. 5, no. 4, pp. 1526-1541, Dec. 2017

[87] X. Wang and F. Blaabjerg " Harmonic stability in power electronic based power systems: concept, modeling, and analysis," *IEEE Trans. Smart Grid*, 2018, early access.

[88] Y. Wang, X. Wang, F. Blaabjerg, and Z. Chen, "Small-signal stability analysis of inverter-fed power systems using component connection method," *IEEE Trans. Smart Grid*, 2017, early access.

[89] G. Gaba, S. Lefebver, and D. Mukhedkar, ''Comparative analysis and study of the dynamic stability of AC/DC systems,'' *IEEE Trans. Power Syst.*, vol. 3, no. 3, pp. 978-985, Aug. 1988.

[90] J. Sun, "Impedance-based stability criterion for grid-connected inverters," *IEEE Trans. Power Electron.*, vol. 26, no. 11, pp. 3075–3078, Nov. 2011.

[91] S. Shah and L. Parsa, "Impedance modeling of three-phase voltage source converters in DQ, sequence, and phasor domains," *IEEE Trans. Energy Convers*., vol. 32, no. 3, pp. 1139-1150, Sep. 2017.

[92] G. P. Tolstov, Fourier Series. Englewood Cliffs, NJ, USA: Prentice-Hall, 1962.

[93] D. G. Holmes and T. A. Lipo, Pulse width modulation for power converters: principles and practice. Piscataway, NJ, USA: Wiley, 2003.

[94] S. Shah and L. Parsa, "Sequence-domain transfer matrix model of three phase voltage source converters," *in Proc. of IEEE PES GM Conference*, USA, 2016, pp. 1-5.

[95] L. Harnefors, R. Finger, X. Wang, H. Bai, and F. Blaabjerg, "VSC input-admittance modeling and analysis above the nyquist frequency for passivity-based stability assessment," *IEEE Trans. Ind. Electron.*, vol. 64, no. 8, pp. 6362-6370, Aug. 2017.

[96] A. Rygg, M. Molinas, C. Zhang, and X. Cai, "A modified sequence-domain impedance definition and its equivalence to the dq-domain impedance definition for the stability analysis of AC power electronic systems," *IEEE Trans. Emerg. Sel. Topics Power Electron.*, vol. 4, no. 4, pp. 1383-1396, Dec. 2016.

[97] E. Ebrahimzadeh, F. Blaabjerg, X. Wang, C. L. Bak, "Harmonic instability source identification in large wind farms," *in Proc. of IEEE PES GM Conference*, USA, 2017, pp. 1-5.

[98] E. Ebrahimzadeh, F. Blaabjerg, X. Wang, and C. L. Bak "Bus participation factor analysis for harmonic instability in power electronics based power systems," *IEEE Trans. Power Electron*., 2018, early access.

[99] F. Gao, X. Zheng, S. Bozhko, C. I. Hill, and G. Asher, "Modal analysis of a PMSG-based DC electrical power system in the more electric aircraft using eigenvalues sensitivity," *IEEE Trans. Transport. Electrific*, vol. 1, no. 1, pp. 65-76, Jun. 2015.

[100] Z. Shuai, Y. Hu, Y. Peng, C. Tu and Z. J. Shen, "Dynamic stability analysis of synchronverter-dominated microgrid based on bifurcation theory," *IEEE Trans. Ind Electron.*, vol. 64, no. 9, pp. 7467-7477, Sep. 2017.

[101] Y. Wang, X. Wang, F. Blaabjerg, and Z. Chen, "Harmonic instability assessment using state-space modeling and participation analysis in inverter-fed power systems," *IEEE Trans. Ind Electron.*, vol. 64, no. 1, pp. 806-816, Jan. 2017.

[102] L. P. Kunjumuhammed, B. C. Pal, C. Oates, and K. J. Dyke, "Electrical oscillations in wind farm systems: analysis and insight based on detailed modeling," *IEEE Trans. Sustain. Energy*, vol. 7, no. 1, pp. 51–62, Jan. 2016.

[103] J. Conroy and R. Watson, "Aggregate modelling of wind farms containing full-converter wind turbine generators with permanent magnet synchronous machines: transient stability studies," *IET Renew. Power Gener.*, vol. 3, no. 1, pp. 39-52, Mar. 2009.

[104] N. C. Yang and M. D. Le, "Three-phase harmonic power flow by direct ZBUS method for unbalanced radial distribution systems with passive power filters," *IET Renew. Power Gener.*, vol. 10, no. 13, pp. 3211-3219, Jul. 2016.

[105] T. Tarasiuk and M. Gorniak, "Load sharing in ship microgrids under non-sinusoidal conditions—case study," *IEEE Trans. Energy Convers.*, vol. 32, no. 2, pp. 810-819, Jun. 2017.

[106] K. L. Lian and T. Noda, "A time-domain harmonic power-flow algorithm for obtaining non-sinusoidal steady-state solutions," IEEE Trans. Power Deliv., vol. 25, no. 3, pp. 1888-1898, Jul. 2010.

[107] S. K. Chaudhary, "Control and protection of wind power plants with VSC-HVDC connection," PhD Thesis, Aalborg University, Aalborg, Denmark, 2011.

[108] S. Skogestad and I. Postlethwaite, Multivariable feedback control: analysis and design, New York: Wiley, 2000.

[109] Y. Cui and X. Wang, "Modal frequency sensitivity for power system harmonic resonance analysis," *IEEE Trans. Power Del.*, vol. 27, no. 2, pp. 1010–1017, Apr. 2012.

[110] E. Ebrahimzadeh, F. Blaabjerg, X. Wang, and C. L. Bak, "Dynamic resonance sensitivity analysis in wind farms," in *Proc. of IEEE PEDG Conference*, Brazil, 2017, pp. 1-5.

[111] K. N. B. M. Hasan, K. Rauma, A. Luna, J. I. Candela, and P. Rodriguez,"Harmonic compensation analysis in offshore wind power plants using hybrid filters," *IEEE Trans. Ind. Appl.*, vol. 50, no. 3, pp. 2050–2060, May/Jun. 2014.

[112] E. Ebrahimzadeh, F. Blaabjerg, X. Wang, and C. L. Bak, "Reducing harmonic instability and resonance problems in PMSG based wind farms," *IEEE Trans. Emerg. Sel. Topics Power Electron.*, 2018, early access.

[113] E. Ebrahimzadeh, F. Blaabjerg, X. Wang, and C. L. Bak, "Multi-objective optimization of large wind farm parameters for harmonic instability and resonance conditions," *in Proc. of IEEE COMPEL Conference*, Norway, 2016, pp. 1-8.

ISSN (online): 2446-1636
ISBN (online): 978-87-7210-173-6

AALBORG UNIVERSITY PRESS